Key - note - paper S

A Review of Measuring Methods for Surface Integrity

Michael Field, John F. Kahles, and John T. Cammett, Metcut Research Associates Inc., Cincinnati, Ohio, USA

Introduction

Within recent years, on a worldwide basis, designers and manufacturers of critical and highly stressed structural components have been engaged in a serious reassessment of the pronounced influence of manufacturing methods on mechanical properties and service performance as a result of the type of surface produced. This has come about because of increased demands for reliability and safety, unusual service requirements, development of and need for understanding of new manufacturing processes, and the availability of extensive sets of surface integrity data.

In order to specify and manufacture surfaces having a high degree of integrity, it has become essential to understand the need for the interdisciplinary application of metallurgy, machinability, and mechanical testing to the production of surfaces. In meeting this special need, the discipline known as surface integrity has come to be recognized as a meaningful technology concerned with the development of unimpaired or enhanced surfaces. Surface integrity is achieved by using manufacturing processes which are carefully selected and controlled based upon the evaluation of significant engineering properties.

The results of high cycle fatigue tests alone are supportive of the need for keen interest on the part of designers and manufacturing engineers in the subject of surface integrity. See Tables I and II. Table I lists a wide variety of high strength materials which show surface sensitivity in fatigue testing to the specific parameters selected for grinding. An examination of the data indicates that currently used conventional grinding procedures may in fact be abusive. These data are supportive of the concern which is often expressed when conventional grinding is specified for the manufacture of critical parts. In reviewing Table II one can readily appreciate the problem of the designer who is now confronted with many values of the endurance limit of Inconel 718 at 10^7 cycles ranging from 22,000 to 78,000 lb./in.^{2} and with each one dependent upon the selection and use of specific manufacturing practices. This situation enhances greatly the need for a much closer coordination between designers and manufacturing engineers.

TABLE I

Fatigue Strength After Surface Grinding

Alloy	Type of Grind	Endurance Limit in Bending 10^7 Cycles, lb./in.^{2}
4340 Steel, Q & T, 50 R_c	Gentle	102,000
	Conventional	70,000
	Abusive	62,000
300 M Steel, Q & T, 53 R_c	Gentle	122,000
	Conventional	65,000
	Abusive	62,000
Grade 300 Maraged Steel, Aged, 54 R_c	Gentle	105,000
	Conventional	82,000
	Abusive	85,000
Ti-6Al-4V, Beta Rolled, 32 R_c	Gentle	62,000
	Abusive	13,000
Ti-6Al-6V-2Sn, Aged, 42 R_c	Gentle	65,000
	Conventional	30,000
	Abusive	20,000
Inconel 718, Aged, 44 R_c	Gentle	60,000
	Conventional	24,000
AF 95, Aged, 50 R_c	Gentle	75,000
	Conventional	24,000
	Abusive	26,000

The general subject of surface integrity was presented at the 21st General Assembly of CIRP, September, 1971 [1]. In view of the wide interest in surface technology, CIRP considered it appropriate to present a paper on techniques for measurement of surface properties. Specifically, the purpose of this paper is to discuss the nature of surface layers from an engineering point of view and to review the techniques and practices currently being used to evaluate and control surface integrity.

TABLE 2

Effect of Machining and Peening on Fatigue Strength of Inconel 718, Aged, 44 R_c

Operation	Endurance Limit in Bending 10^7 Cycles, lb./in.^{2}	Endurance Limit % of Gentle Grind
Surface Grind — Gentle	60,000	100
Surface Grind — Conventional	24,000	40
Turning — Gentle	60,000	100
Turning — Abusive	60,000	100
ECM — Standard	39,000	65
ECM — Off-Standard	39,000	65
ECM — Standard + Peen	78,000	130
ECM — Off-Standard + Peen	67,000	112
EDM — Finish	22,000	37
EDM — Rough	22,000	37
EDM — Finish + Peen	66,000	110
EDM — Rough + Peen	75,000	125
Electropolish	42,000	70
Electropolish + Peen	78,000	130

The nature of a surface can be defined by a consideration of 1) surface topography and 2) surface and subsurface metallurgy. The subject of surface topography or surface texture has been studied extensively for a considerable number of years, and therefore a review of this subject will not be attempted here. Suffice it to say that there are well known and widely used contact and noncontact methods for determining surface topography [2]. The surface contact method usually employs a stylus which is translated over either a line or an area of the surface. The surface contour obtained from the motion of the stylus in the simplest form may be given as the centerline arithmetic average. In addition, the surface profile may be recorded in various degrees of sophistication. The data of the surface profile can be put into a computer whose output has been either a representation of the surface by contour mapping [3] or a representation of a surface by radii of curvature mapping [4]. Noncontact surface topography measurements have also been produced by optical as well as by interferometer and holography instruments [2].

Surface topography is extremely important in studies of friction, wear, fretting, bearings, etc., but these subjects will not be treated in detail in this paper. Instead, we shall concern ourselves mainly with the structural applications of materials and their related properties. The topography of surfaces has important functions in the application of structural materials, but generally the surface finishes involved in producing structural components are much rougher. For example, on bearings the surface finish specified is generally of the order of 1 to 10 microinches CLA. In contrast, the surface rougness of structural components varies from 15 to 200 CLA. Figure 1 shows the range and average values of surface finish produced

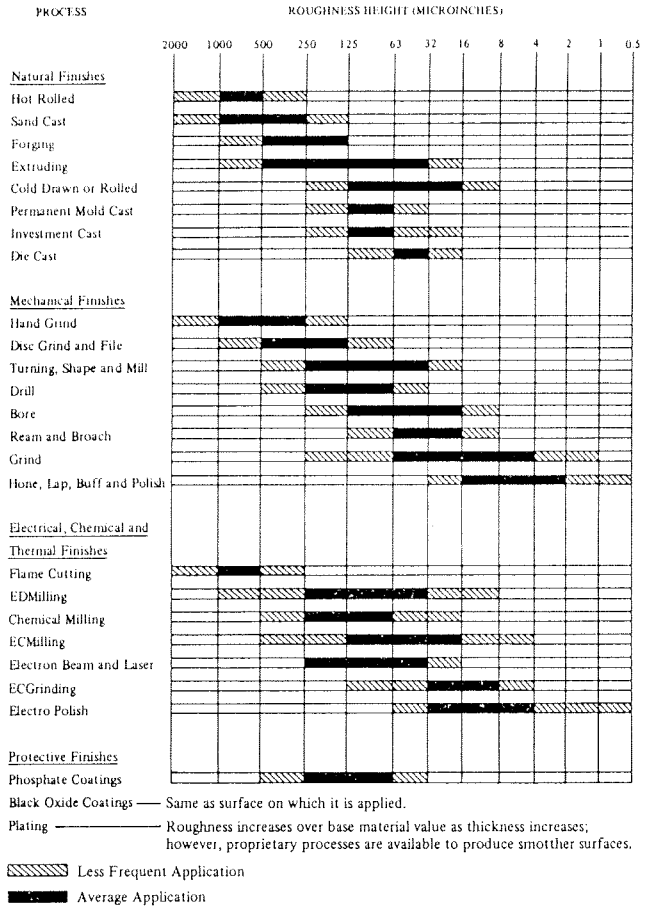

Fig. 1. Surface roughness produced by common production methods.

by a variety of machining and other processing practices. With regard to surface finish, a limited amount of fatigue testing accomplished recently shows that in the range of 10 to 125 microinches CLA surface finish cannot of itself be used as a measure or control of surface integrity for structural components.

While much more can be said about practical aspects of the measurement and control of surface finish, the specific purpose of this paper is to review techniques for determining the surface and subsurface metallurgy characteristics of materials and to relate them to important properties such as distortion, static and dynamic strength, and stress corrosion.

Defining the Surface Integrity Problem

Before applying surface integrity technology, one must first decide whether a surface integrity problem actually exists. The control of surface integrity generally adds cost to the manufacturing process, and hence surface integrity should not be considered unless a potential problem exists or may be considered as a possibility. There are certain applications where surface integrity may not be a problem. In fabricating a machine tool bed, steel plate is flame cut and welded, usually subject to design requirements involving such low stresses that failures may never be a problem. On the other hand, surface integrity must be considered in the manufacture of highly stressed components used in applications involving high cost, predictable component life, and human safety. If surface integrity is a problem, then the pertinent surface characteristics and the affected engineering properties of the material must be monitored. In some applications, such as antifriction bearings, the major mode of failure may be contact fatigue which, in turn, may be related to the presence of microcracks and untempered martensite. For example, in the grinding of bearing races made of hard bearing steels, it is necessary to monitor the microcrack formation, the presence of untempered and overtempered martensite, surface roughness, and component accuracy. On a component such as a gage block where dimensional stability and accuracy are most important, the properties which require monitoring are surface finish, accuracy, and residual stress imposed by the final grinding and lapping processes. Monitoring of residual stress over a period of time is also very important because residual stress relaxation may occur, thereby producing dimensional alterations.

In the case of grinding a cast nickel base alloy component, two very important considerations are the tendency for the grinding operation to generate microcracks and to pull out grain boundary carbides; hence, control must be centered on these factors. In the manufacture of high strength steel structural components, such as airplane landing gear or airplane wing structures, the presence of untempered or overtempered martensite can produce major degradation of the fatigue strength, and hence untempered and overtempered martensite must be carefully monitored and avoided. In grinding of carburized or other hardened gears, there is a tendency to produce microcracks, untempered or overtempered martensite. Here again, processing parameters must be selected so as to avoid these imperfections. In the machining of slender parts which have a tendency to warp, the residual stress in the machining operation must be kept to a minimum because the residual stress is a major factor affecting the distortion of the finished product. The use of a nontraditional machining operation, such as ECM of a nickel base alloy, may produce no undesirable metallurgical alterations or microcracks but may still result in a major depression in fatigue strength. Here, then, fatigue strength is the significant material property that should be investigated.

Experimental Approach for Defining Surface Integrity Effects

An experimental procedure has been developed for approaching surface integrity problems [5]. The procedure specifies obtaining three types or levels of data: 1) The Minimum Surface Integrity Data Set, 2) The Standard Surface Integrity Data Set, and 3) The Extended Surface Integrity Data Set.

A. Minimum Surface Integrity Data Set

Developing the *Minimum Surface Integrity Data Set* is the least expensive approach and should therefore be considered first in screening tests of surfaces. The *Minimum Surface Integrity Data Set* is essentially metallographic information supplemented with microhardness measurements and conventional surface finish measurements:

Minimum Surface Integrity Data Set
1. Surface finish
2. Macrostructure (10X or less)
a. Macrocracks
b. Macroetch indications
3. Microstructure
a. Microcracks
b. Plastic deformation
c. Phase transformations
d. Intergranular attack
e. Pits, tears, laps, protrusions
f. Built-up edge
g. Melted and redeposited layers
h. Selective etching
4. Microhardness

B. Standard Surface Integrity Data Set

This set of data is designed to provide more in-depth data for the more critical applications which are influenced by surface integrity:

Standard Surface Integrity Data Set
1. Minimum Surface Integrity Data Set
2. Fatigue tests (screening)
3. Stress corrosion tests
4. Residual Stress and distortion

Data summarized in Figure 2 are taken from a Standard Surface Integrity Data Set produced in grinding of 4340 steel, quenched and tempered to 50 R_c.

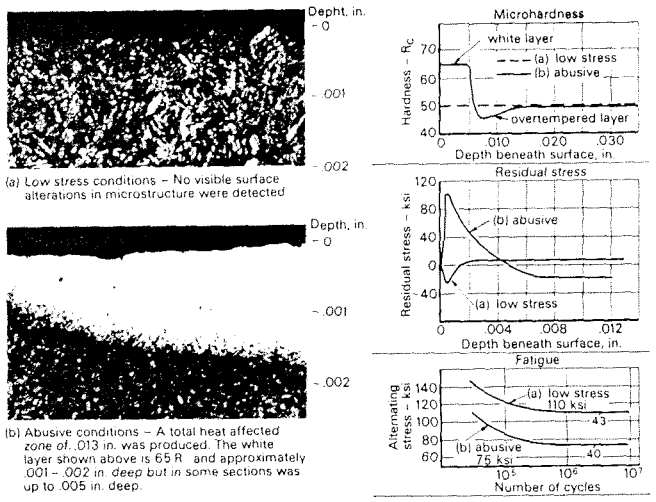

Fig. 2. Surface characteristics produced by grinding AISI 4340 steel, quenched and tempered, 50 R_c.

C. Extended Surface Integrity Data Set

The *Extended Surface Integrity Data Set* provides data gathered from statistically designed fatigue programs and yields data suitable for detailed designing:

Extended Surface Integrity Data Set
1. Standard Surface Integrity Data Set
2. Fatigue tests (extended to obtain design data)
3. Additional mechanical tests
a. Tensile
b. Stress rupture
c. Creep
d. Other specific tests (e.g., bearing performance, sliding friction evaluation, sealing properties of surfaces)

Techniques for Surface Integrity Measurements

Properties which may require investigation in order to establish surface integrity include surface topography, surface metallurgy, mechanical properties, surface chemistry, and other engineering properties. The techniques for evaluation of these properties are separated into standard and specialized techniques. The standard techniques are those which generally are employed first, while the specialized techniques are used later in more extensive investigations. Table III provides a convenient summary for reference purposes.

Techniques for Evaluation of Surface Metallurgy

A. Metallurgical Evaluation

1. Metallurgical Sectioning and Special Preparation Techniques

Special metallographic techniques are necessary for studying surface phenomena. The surface microstructure alterations are generally very shallow, usually of the order of .001-.003 in. Under very abusive conditions, alterations as deep as .005-.015 in. have been noted. Often significant microstructure alterations, microcracks, or flaws as shallow as .0001 in. in depth are developed during material removal processing. Thus, it is necessary to employ sectioning, mounting and other metallographic techniques which do not alter or destroy the pertinent surface and which maintain high edge retention. One successful technique consists of the application of vacuum epoxy mounting as outlined in the following [6]:

Mounting Technique and Metallographic Preparation for Edge Retention

1. Samples are sectioned from the workpiece in a manner which leads to the least possible distortion or burring. Bandsawing or hacksawing is preferred. A minimum of .030 in. is then removed from the cut surface using a 120 grit silicon carbide paper on a low speed polisher.
2. Copper molds (or tubes), 1-¼ in. inside diameter by 2-¾ in. high, are placed on a pallet approximately 5 in. in diameter. The inner surface of the molds and surface of the pallet are previously sprayed with a silicone releasing agent.
3. After placing a metallurgical specimen in a mold, a mixture of epoxy resin, hardener, and pelletized aluminum oxide, sufficient to produce a layer of ¼ to ⅜ in. in depth, is poured over the specimen. The ratio of resin to hardener is 4 to 1. The amount of pellets added is in the range of 10-15 grams. The hardness or abrasive level of the pelletized material used (low, medium, or high fired) is strictly a function of the alloy to be prepared and its hardness characteristics.
4. The pallet containing the molds is placed in a vacuum chamber (at a vacuum of 1×10^{-2} to 1×10^{-3} torr) in order to degas the mixture, thereby improving the adherence of the epoxy and pellets to the surface of the specimen. When vigorous bubbling of the mixture decreases after vacuum impregnation, sufficient resin and hardener (4 to 1 ratio) is added to produce a mount approximately 1 in. high.
5. The mounts are cured at a temperature not greater than 70° F for approximately 10 hours. Casting of the mounts is accomplished during the latter portion of the laboratory workday, so that curing occurs over night.
6. After curing, they are placed in an oven at a temperature of 150° F for a period of one hour, after which they are removed from the molds. See Figure 3.
7. Approximately .020 in. of stock is then removed from the as-mounted metal surface on a positive positioning automatic polishing unit, using the side of a 1 in. by 1 in. by 13 in. aluminum oxide 320 grit grinding wheel as the grinding medium. Water is used as a coolant.
8. Subsequent rough grinding is performed wet on silicon carbide papers or equivalent ranging from 240 to 600 grit.
9. For steels, and nickel and cobalt base superalloys, the intermediate polish is performed on an automatic polisher using

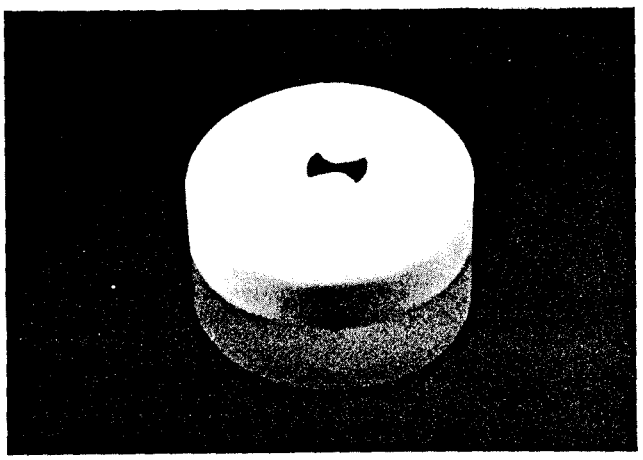

Fig. 3. A 1¼" diameter metallographic mount prepared by the vacuum epoxy method. The white layer contains aluminium oxide pellets.

TABLE 3

Techniques for Surface Integrity Measurements

Property	Standard Techniques	Specialized Techniques
Surface Topography	Contact (Tracer Point or Stylus Measurement) — Linear Traverse or Area Traverse	Noncontact Measurements — Optical Microscopy Interference Microscopy, etc. Three Dimensional Surface Profile by Combination of Roughness Measurement and Computer Plotting Scanning Electron Microscopy
Surface Metallurgy		
Microstructure	Metallurgical Sectioning — Optical Microscopy	Transmission Electron Microscopy
Microhardness	Microhardness Testing — Knoop or Vickers Indenter	
Microcracks and Crevice-Like Defects	Metallurgical Sectioning — Optical Microscopy Nondestructive — Macroetching Penetrant Inspection etc.	Scanning Electron Microscopy Nondestructive — Eddy Current Ultrasonic etc.
Static Mechanical Properties		
Tensile Strength & Ductility	Tensile Testing	
Stress Rupture & Creep	Creep Testing	
Residual Stress	X-Ray Diffraction Layer Removal — Curvature Measurement	
Stress Corrosion	*Steels & Aluminium:* Constant Prestress with Alternate Immersion in Salt Solution and Air *Titanium:* Specimen Coated with Salt or Halide and Exposed to High Temperature and Stress	Stress Corrosion Crack Propagation Testing
Fracture Toughness		Fracture Toughness Testing
Dynamic Mechanical Properties		
High Cycle Fatigue	Bending Fatigue Testing, A* = ∞	Axial Fatigue Testing, A* = 0.95
Low Cycle Fatigue	Bending Fatigue Testing, A = ∞	Axial Fatigue Testing, A = 0.95
Surface Chemistry	Electron Microprobe Analysis Dissolution of the Surface Layer by Chemical or Electrochemical Etching followed by Spectroscopy, Spectrophotometry, etc.	Electron Spectroscopy — Electron Spectroscopy for Chemical Analysis (ESCA) Auger Spectroscopy Ion Spectroscopy — Ion Scattering Spectrometry Ion Probe Mass Spectroscopy
Other Engineering Properties Friction Wear Fretting Galling & Seizing Corrosion Reflectivity Electrical Properties Etc.	A variety of standard and specialized techniques have been developed to evaluate these properties for specific applications.	

* A = ratio of dynamic/static stress.

a polishing cloth with a soft nap texture and 6 micron diamond paste. The final polish is achieved using deep nap or pile cloth similar to billiard cloth with a suspension of 0.1 micron or finer aluminum oxide in water.

Titanium and refractory alloys require an etch-polish cycle (using a slurry of hydrogen peroxide, water, and 0.1 micron or finer aluminum oxide) which is accomplished between a diamond polish and a final polish procedure. The final polish for titanium and refractory alloys is accomplished on a vibratory polisher using a deep pile cloth with a suspension of 0.1 micron or finer aluminum oxide in water.

10. Samples are etched by swabbing. Examples of some typical etchants used are given below:

Material	*Etchant*
Steels	2% HNO_3 & 98% Denatured Anhydrous Alcohol
Nickel Base Alloys	100 ml. HCl, 5 gm. $CuCl_2 \cdot 2\ H_2O$, and 100 ml. Denatured Anhydrous Alcohol
Titanium Alloys	2% HF & 98% H_2O or 2% HF, 3% HNO_3, & 95% H_2O

2. Microhardness Determination

Microhardness determinations can be made on the previously described metallurgical mounts using a microhardness tester with either a Knoop or Vickers indenter. Microhardness studies are extremely important for identifying microconstituents such as untempered and overtempered martensite and for determining the possible overall effects of specific material removal operations. Examples of microhardness variations include:

a) Identification of untempered martensite; for example, microhardness of over 60 R_c compared to base hardness of 50 R_c, Figure 2.

b) Identification of overtempered martensite, Figure 2.

c) A soft layer of resolutioned austenite (austenite reversion) in a maraging steel when improperly drilled with a dull drill as shown in Figure 4.

d) Identification of surface softening produced by chemical milling, Figure 5. (Surface softening is also common in electrochemical machining.)

e) Identification of plastic deformation and work hardened zones in operations such as drilling and reaming, Figure 6.

In determining the microhardness using a Knoop indenter, we generally employ a 100 gram load. With this load, accurate hardness readings can be made to within .001 in. of the surface without producing edge yielding. Surface hardness readings to within .0005 in. of the surface may be made using 25-50 gram loads, but extreme care must be taken with these light loads. It is recommended that if the light load is used, hardness readings should also be taken at a considerable distance

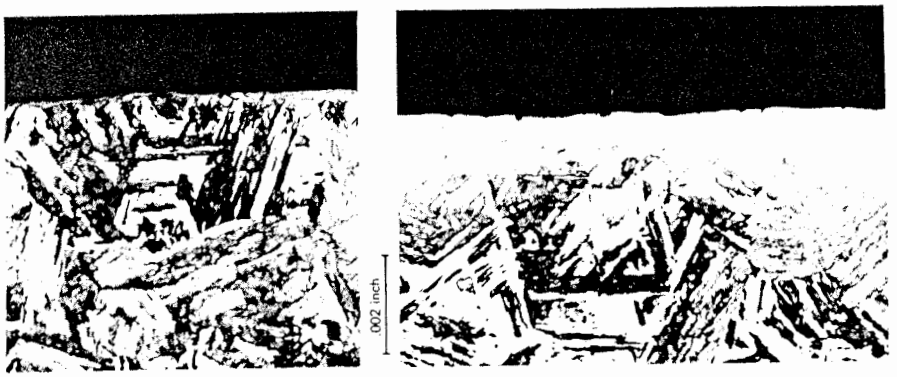

a) Gentle conditions. Very thin trace of cold work may be seen on the surface.

b) Abusive conditions. An overaged or resolutioned layer .001" deep at 37 R_C is found on the surface. Total affected depth is approximately .002".

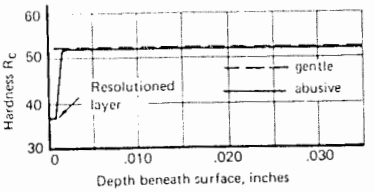

Fig. 4. Surface characteristics of 18% nickel-maraging steel (grade 250, aged, 52 R_C) produced by drilling.

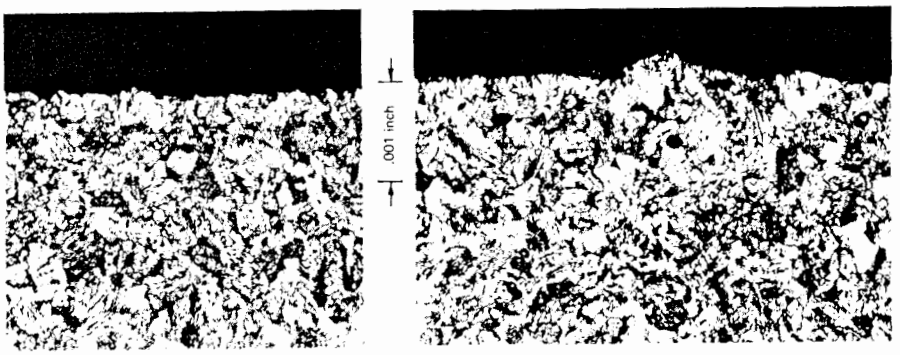

a) Gentle conditions. No visible surface effects other than shallow hardness loss. Surface finish 35 AA.

b) Abusive conditions. Slight surface roughening plus indicated hardness loss less than .002" deep. Surface finish 120 AA.

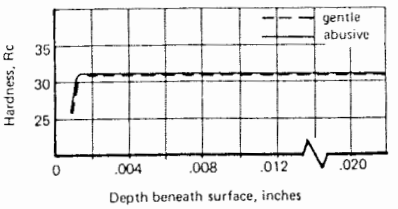

Fig. 5. Surface characteristics of 4340 steel (annealed, 31-36 R_C) produced by CHM.

Fig. 6a. Drilling 4340, 51 R_C, with dull drill white (untempered martensite) layer.

Fig. 6c. Reaming 4340, 53 R_C, with dull reamer tears from built-up edge.

Fig. 6b. EDM on D2 tool steel, 61 R_C, redeposited metal on surface.

from the edge and compared with loads of 100 and 500 gram Knoop readings. We find that it is desirable to convert Knoop readings to Rockwell C readings for more ready appreciation of the relative hardnesses involved.

3. *Microscopic Examination*

Various types of microscopy are available for evaluation of surface metallurgy including optical microscopy, scanning electron microscopy (SEM), and transmission electron microscopy (TEM). Optical microscopy is the least expensive and the most widely applicable method. It is advisable to examine metallurgical mounts first in the unetched condition which accentuates surface profile, microcracks, inclusions, voids, and crevice-like defects. After etching, specimens are reexam-

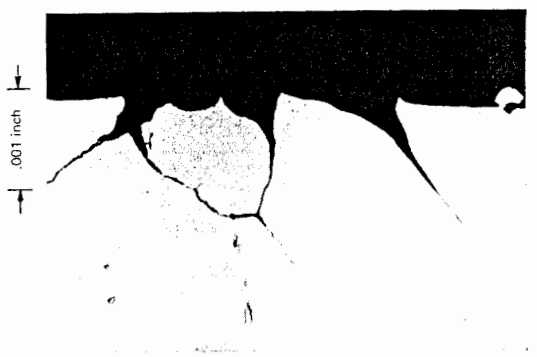

Fig. 6d. ECM of waspaloy, aged, 40 R_C, intergranular attack.

ined for the aforementioned imperfections or characteristics as well as for microstructure identification and grain boundary conditions. Specimens should be scanned at both high and low magnifications. It is common practice to observe the surface at magnifications of 1000 × in order to resolve many of the surface effects which have been found to be significant, see Figures 4, 5 and 6.

Scanning electron microscopy enables one to look directly at the machined surface without replicating. The scanning electron microscope, a relatively new instrument, has been applied in defining surface topography and in discovering and identifying cracks, crevices, and other topographical characteristics. Ramalingam and Black have discovered microcracks on both ground and milled surfaces [7]. Betz has been studying the surface topography and, in particular, the surface roughness imperfections produced through the formation of the built-up edge [8].

SEM provides a magnification capability from approximately 20 × to 50,000 × and a resolution of the order of 200 Å. SEM also provides a larger depth of field corresponding to the magnification employed in the observation than can be obtained from other optical instruments. Figure 7 shows the surface topography of an electrical discharge machined surface of Inconel 718 from 20 × to 500 × [9].

TABLE 4

Summary of Possible Surface Alterations Encountered by Metal Removal Processes (6)

Material	Conventional Metal Removal Methods				Nontraditional Removal Methods		
	Milling	Drilling	Turning	Grinding	EDM	ECM	CHM
Steels							
Nonhardenable (1018)	R, PD, L & T			R, PD	R, MCK, RC	R, SE, IGA	R, SE, IGA
Hardenable (Alloy) (4340) (D6ac)	R, PD, L & T MCK, UTM, OTM			R, PD, MCK, UTM, OTM	R, MCK, RC, UTM, OTM	R, SE, IGA	R, SE, IGA
Tool Steel, D2	R, PD, L & T MCK, UTM, OTM			R, PD, MCK, UTM, OTM	R, MCK, RC, UTM, OTM	R, SE, IGA	R, SE, IGA
Stainless (Martensitic) (410)	R, PD, L & T, MCK, UTM, OTM			R, PD, MCK, UTM, OTM	R, MCK, RC, UTM, OTM	R, SE, IGA	R, SE, IGA
Stainless (Austenitic) (302)	R, PD, L & T			R, PD	R, MCK, RC	R, SE, IGA	R, SE, IGA
Precipitation Hardening (17-4PH)	R, PD, L & T, OA			R, PD, OA	R, MCK, RC, OA	R, SE, IGA	R, SE, IGA
Maraging (18 % Ni) (250 Grade)	R, PD, L & T, RS, OA			R, PD, RS, OA	R, RC, RS, OA	R, SE, IGA	R, SE, IGA
Nickel and Cobalt Base Alloy							
Inconel 718, Rene' 41, HS 31, IN 100	R, PD, L & T, MCK			R, PD, MCK	R, MCK, RC	R, SE, IGA	R, SE, IGA
Titanium Alloy							
Ti-6Al-4V	R, PD, L & T			R, PD, MCK	R, MCK, RC	R, SE, IGA	R, SE
Refractory Alloy							
Moly TZM	R, L & T, MCK			R, MCK	R, MCK	R, SE, IGA	R, SE
Tungsten (Pressed and Sintered)	R, L & T, MCK			R, MCK	R, MCK	R, SE, MCK, IGA	R, SE, MCK, IGA

TABLE 5

Surface Hardness Changes that May be Encountered by Metal Removal Processes (6)

Material	Conventional Metal Removal Methods				Nontraditional Removal Methods		
	Milling	Drilling	Turning	Grinding	EDM	ECM	CHM
Steels	PD, UTM: Increase; PD, OTM, RS, OA: Decrease			PD, UTM: Inc.*; PD, OTM, RS, OA: Dec.*	RC-Inc.*, UTM-Inc.*, OTM-Dec.*, RS-Dec.*, OA-Dec.*	Decrease	Decrease
Nickel and Cobalt Base Super Alloys	PD-Increase			PD-Inc.*	RC-Inc.*	Decrease	Decrease
Titanium Alloys	PD-Increase			PD-Inc.*	RC-Inc.*	Decrease	Decrease
Refractory Alloys (Moly TZM, Tungsten)					No Change	Decrease	Decrease

* Inc. — Increase
Dec. — Decrease

Code for the Surface Alterations Presented in Tables 4 and 5

R — Roughness of Surface
PD — Plastic Deformation and Plastically Deformed Debris
L & T — Laps and Tears and Crevice-Like Defects
MCK — Microcracks
SE — Selective Etch
IGA — Intergranular Attack
UTM — Untempered Martensite
OTM — Overtempered Martensite
OA — Overaging
RS — Resolution or Austenite Reversion
RC — Recast, Respattered Metal, or Vapor Deposited Metal

The application of transmission electron microscopy in the study of surfaces is somewhat limited. With regard to surface integrity studies, TEM has been used for the investigation of fracture surfaces and fracture origins. TEM of surfaces requires the use of a replicating technique. With this technique, a cellulose acetate sheet moistened with methyl acetate is placed on the surface; and, after drying in place, it is peeled from the surface. The plastic replica is usually shadowed with a film of chromium and a support film of carbon. The film is then removed from the plastic and placed in the electron microscope [10].

4. Types of Surface Alterations Produced in Various Machining Operations

Some common types of surface alterations which are produced on surfaces by major machining operations are as follows:

a) Surface roughness
b) Plastic deformation
c) Tears, laps, and crevice-like defects associated with built-up edge
d) Plastically deformed debris associated with grinding
e) Microcracks
f) Intergranular attack and selective etching
g) Microhardness change
h) Phase transformations such as formation of untempered martensite
i) Overaging
j) Resolutioning or austenite reversion
k) Recast metal
l) Spattered or vapor deposited metal
m) Friction welding of high speed tool steel
n) Recrystallization

Most of the above surface alterations result from high temperatures, high forces, and plastic deformation produced during the machining processes. It is advisable to become acquainted with the possible types of surface alterations resulting from a combination of various metal removal methods and specific materials [1]. A summary of the possible surface alterations is given in Table 4 [6]. The surface hardness alterations that may be encountered as a result of various metal removal processes on different materials are given in Table 5 [6]. Typical photomicrographs showing surface alterations and microhardness changes on a variety of conventional and nonconventional machining operations are shown in Figures 2, 4, 5 and 6.

B. Nondestructive Test Methods and Applications

The principal nondestructive methods for evaluating surface integrity and subsurface characteristics which pertain to surface integrity are listed in Table 6 along with their applications. face integrity are listed in Table 6 along with their applications [11]. Table 7 lists the various aspects of surface integity and the analytical techniques which are prevalent in industry or which show potential but require further development work. Destructive techniques are also listed in Table 7 for comparison [1, 11].

Almost all manufactured parts are subjected to some sort of visual inspection, sometimes employing optical aids. This technique is limited to detection of visible macrocracks and other surface defects. The use of dye penetrants and magnetic particle inspection techniques improves the resolution of small crack-like defects and sometimes permits detection of flaws which have been smeared over by the finishing operation

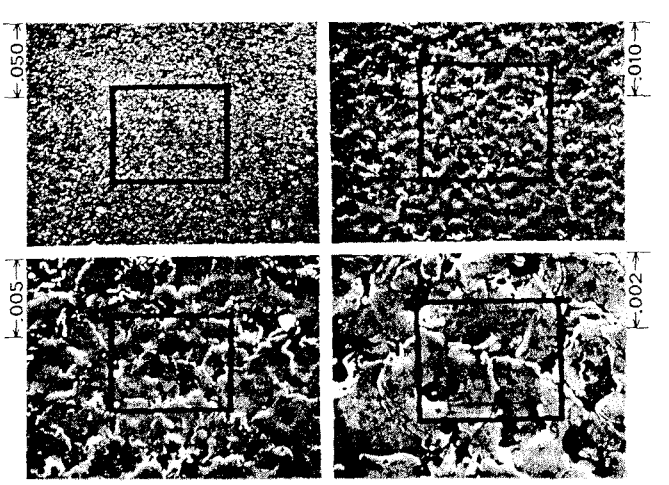

Fig. 7. Scanning electron photomicrograph. EDM of inconel 718, STA-finishing [9].

TABLE 6

Nondestructive Techniques for Detecting Surface Inhomogeneities in Metals (11)

Technique	Application	Status
1. Visual Inspection	Surface Defects	Widely Employed
2. Automatic Optical Scanning	Surface Defects	Specialized
3. Dye Penetrant	Surface Defects	Widely Employed
4. Magnetic Particle	Surface Defects	Widely Employed
5. Acid Macroetch	Crack Detection	Widely Employed
	Surface Phase Transformations	Widely Employed
	Redeposited & Resolidified Metal	Widely Employed
6. Eddy Current	Surface Defects	Widely Employed
	Inclusion & Subsurface Defects	Widely Employed
	Surface Hardness Changes	Specialized
	Plastic Deformation	Specialized
	Surface Phase Transformation	Needs Development
	Subsurface Fatigue	Needs Development
	Residual Stress Analysis	Needs Development
7. Ultrasonic Pulse Echo	Inclusions & Subsurface Defects	Widely Employed
	Surface Defects	Specialized
8. Ultrasonic Velocity	Residual Stress Analysis	Specialized
	Surface Phase Transformation	Needs Development
	Plastic Deformation	Needs Development
9. Ultrasonic Attenuation	Recrystallization & Grain Growth	Specialized
	Residual Stress Analysis	Needs Development
10. High Frequency Ultrasonic	High Resolution of Surface Defects	Specialized
11. X-Ray Radiography	Subsurface Defects	Widely Employed
12. X-Ray Diffraction	Residual Stress Analysis	Widely Employed
	Surface Phase Transformation	Specialized
13. X-Ray Spectroscopy	Composition Changes	Needs Development
14. Neutron Radiography	Subsurface Defects	Specialized
15. Gamma Radiography	Subsurface Defects	Specialized
16. Radioactive Gas Penetrant	Surface Defects	Needs Development
	Recrystallization & Grain Growth	Needs Development
	Plastic Deformation	Needs Development
	Subsurface Defects	Needs Development
17. Surface Electrical Resistance	Surface Defects	Needs Development
	Surface Phase Transformation	Needs Development
18. Beta Backscatter	Surface Hardness Changes	Needs Development
	Plastic Deformation	Needs Development
19. Electrochemical Potential	Residual Stress Analysis	Needs Development
20. Laser Probe Mass Spectrometry	Surface Composition	Needs Development

on the part. Automatic optical scanning equipment has been developed to replace visual inspection on mass produced parts, but this does not increase the resolution sufficiently to detect small imperfections.

Parts manufactured from martensitic high strength steel can be visually inspected after an acid macroetch for evidence of untempered or overtempered martensite after grinding or machining [12]. A dilute solution of nitric acid is usually employed which etches the damaged areas so that they may be visually detected. Typically, untempered martensite appears white and overtempered areas appear darker than the background material. A specific etching technique for detecting grinding damage in hardened steel is given in Table 8 [13].

Eddy current and other electromagnetic detectors [14, 15] have been vastly improved in the past few years. Claims have been made that under carefully controlled conditions defects as small as .0001 in. can be detected. For manufacturing purposes, however, eddy current technology has not advanced to this degree of capability.

Research on ultrasonic techniques has extended its utility from defect detection by pulse echo to include measurement of residual stresses, plastic deformation, and other inhomogeneities [16, 17, 18, 19] which may exist at a considerable depth below the surface. The major improvements which make ultrasonic suitable for surface integrity are Raleigh wave transducers which confine the ultrasonic energy to specimen surface layers and new analyzers which measure sonic velocities and energy absorption (attenuation) [18, 19].

The initial use of X-rays in nondestructive testing was radiography. Applications have been expanded to utilize X-ray diffraction techniques for measurement of surface residual stresses (indepth stress measurements still require destructive techniques for complete determination of a residual stress profile), phase identification by diffraction techniques and composition analysis by spectroscopic techniques [20]. Improvements in radiographic inspection have been achieved using gamma rays, although these are limited to special applications [21].

Two new techniques are under development for detection of tiny defects. Accoustic impact is similar to ultrasonic detection, except that the driving frequency is much lower and the resonant vibrations are analyzed instead of the fundamental frequency [22].

Radioactive gas penetrant inspection offers promise for a large improvement in resolving minute defects [23]. Radioactive krypton gas is absorbed in surface defects and inspection is accomplished via autoradiographic or electro-optical scanning. Improvements in resolution by a factor of ten million have been reported [23]. Under high pressure, the radioactive gas may be driven into the metal where it localizes at grain boundaries, microcracks, and inclusions.

By vaporizing microscopic amounts of surface material with a laser beam and analyzing the vapors in a mass spectrometer, surface composition of a specimen can be determined. This technique is currently limited to laboratory experimentation.

Determination of Material Property Effects

There are several important material properties which are surface dependent and hence are affected by the nature of the surface and the manner and severity of processing. These include residual stress and distortion, certain static properties such as tensile and creep rupture strength, fatigue strength, and stress corrosion.

A. Residual Stress and Distortion

Whenever a part is machined by any process, a distinctive and rather complex residual stress pattern is imposed on the surface of the material. For example, the stress may be low at the surface and may increase to a high value immediately below the surface and then may decrease to essentially zero

TABLE 7

Testing Techniques Used to Detect and Locate Surface Inhomogeneities in Metals (1, 11)

Metallurgical inhomogeneity	Nondestructive techniques			Destructive techniques
	Commonly employed	Specialized	Possible with further developments	
Macrocracks	Visual inspection Binocular inspection Magnetic particle Penetrant Eddy current Acid macroetch	Ultrasonic pulse echo Automatic optical scanning	Acoustic impact	Optical metallography
Microcracks	Binocular inspection High sensitivity fluorescent pentrant Magnetic particle	Ultrasonic pulse echo, surface waves and lamb waves	Radioactive gas penetrant High frequency ultrasonic Acoustic impact Surface electrical resistance	Optical metallography Scanning electron microscopy Transmission electron microscopy
Tear, laps & pits	Visual with etch Magnetic particle Eddy current Penetrant	Automatic optical scanning	Radioactive gas penetrant	Optical metallography Scanning electron microscopy
IGA & selective etch		High sensitivity Fluorescent penetrant		Macroetch Optical electron microscopy Transmission electron microscopy
Surface phase transformation (OTM, UTM, resolutioning, etc.)	Macroetch	X-Ray diffraction Magnetic particle	Ultrasonic velocity Surface electrical resistance Eddy current	Optical metallography
Composition (changes oxidation, decarb, etc.)			Laser probe Mass spectrometry X-Ray spectroscopy	Wet chemical analysis Electron microprobe
Surface hardness changes	Superficial hardness testing Ultrasonic hardness testing	Eddy current	Beta backsatter	Microhardness traverse
Redeposited & resolidified metal	Macroetch Visual inspection			Optical metallography
Recrystallization & grain growth		Ultrasonic attenuation	Radioactive gas penetrant	Optical metallography
Plastic deformation (cold work, hot work)	Superficial hardness testing	Eddy current Magnetic particle	Beta backscatter Radioactive gas penetrant Ultrasonic velocity	Optical metallography Microhardness traverse
Inclusion & voids	Ultrasonic pulse echo shear wave, surface wave, and lamb wave Penetrant X-Ray radiography Eddy current Magnetic particle	Gamma radiography Neutron radiography	Radioactive gas penetrant	Optical metallography
Residual stresses	X-Ray diffraction	Ultrasonic velocity	Eddy current Electrochemical potential Ultrasonic attenuation Magneto-absorption	Parting-out Layer removal X-Ray diffraction
Distortion	Visual inspection	Metrology		

at a small distance below the surface. Stresses may be tensile or compressive, and the stressed layer may be shallow or deep. Typical residual stress patterns produced by a variety of machining operations on a single material (4340 steel, $50R_c$) are shown in Figure 8. The area under the residual stress curve which represents the surface layer containing the integrated stress has been found to be proportional to the distortion of a specimen.

A convenient specimen for determining the distortion and residual stress produced in machining is shown in Figure 9. This specimen is ¾ in. wide, 4-¼ in. long, and is .060 in. thick after the test cut. The edges of the specimen are tapered so that the specimen can be clamped to a fixture during the test cut.

A typical distortion curve produced in machining the specimen of Figure 9 is shown in Figure 11. The distortion here is shown as the change in curvature over a length of 3.5 in. using the fixture shown schematically in Figure 10. In this case, the higher the wheel speed and the greater the downfeed in surface grinding, the greater the distortion of the workpiece. The residual stress patterns corresponding to the three downfeeds at 6 000 ft./min. are shown in Figure 12.

B. Residual Stress Determination

There are several ways of determining the residual stress profile introduced by the machining processes. The two most common are X-ray diffraction and layer removal-deflection techniques.

1. X-Ray Diffraction Technique

The X-ray diffraction method makes use of the Bragg equation which relates the distance between a given set of parallel planes of atoms in the metal or crystal to the diffraction angle:

$$n\lambda = 2d \sin \theta \qquad (1)$$

where: n = an integer
λ = wavelength of the X-ray
d = interplanar spacing
θ = diffraction angle

When residual stresses are present, the planes of atoms are either farther apart, as in tension, or closer together, as in

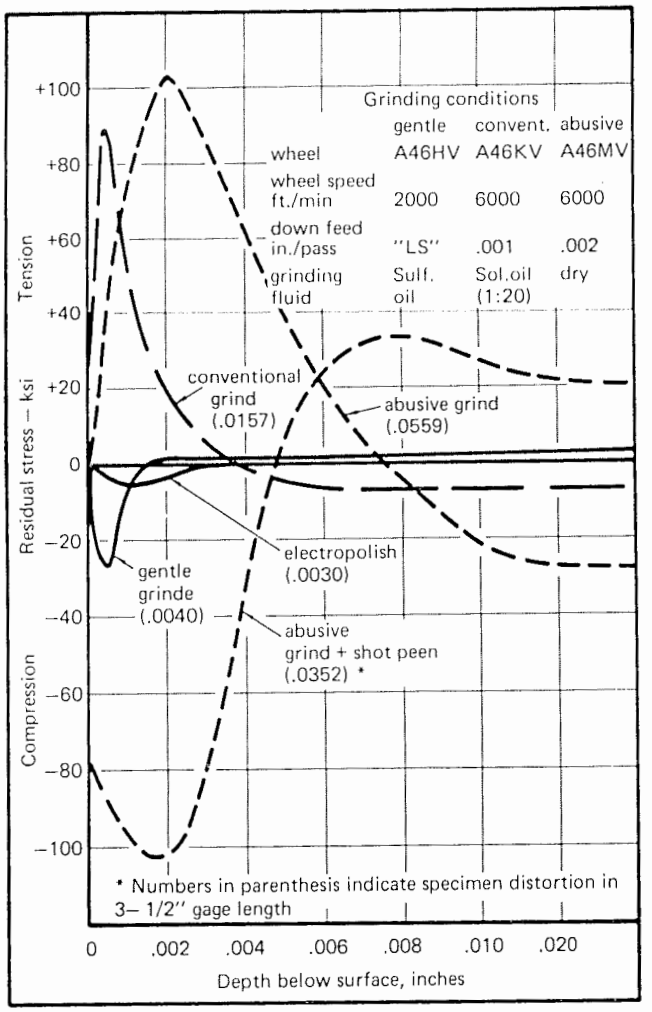

Fig. 8. Residual surface stress in AISI 4340 (quenched an tempered, 50 R_c) produced by surface grinding.

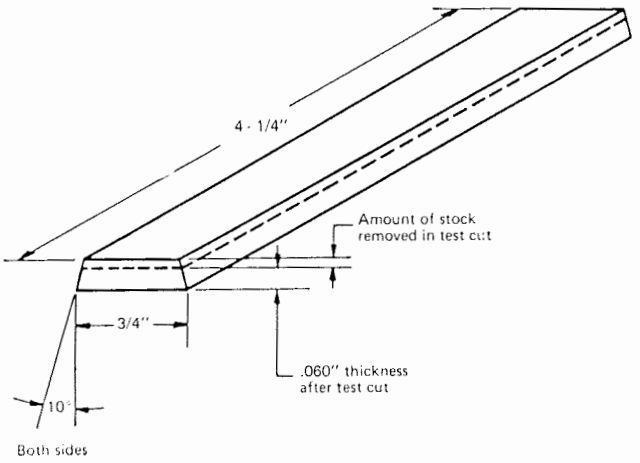

Fig. 9. Distortion and residual stress test specimen.

compression, than found in the stress-free state. The elastic strain associated with these stresses is given by the equation:

$$\varepsilon = \frac{d_s - d_u}{d_u} \tag{2}$$

where: ε = strain
d_u = interplanar distance in stress-free condition
d_s = interplanar distance in stressed cundition

This strain is related to the stress of interest through Hooke's Law and the Poisson ratio:

$$\sigma = -\frac{E}{\nu}\varepsilon \tag{3}$$

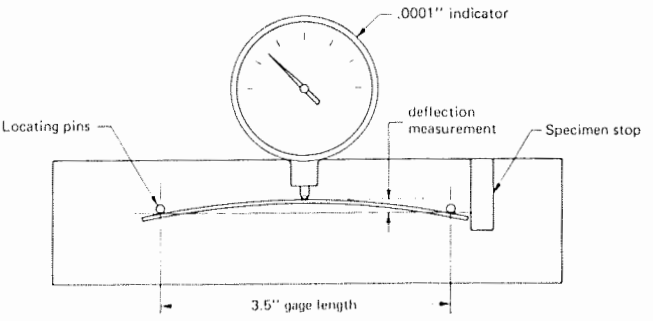

Fig. 10. Deflection measurement fixture.

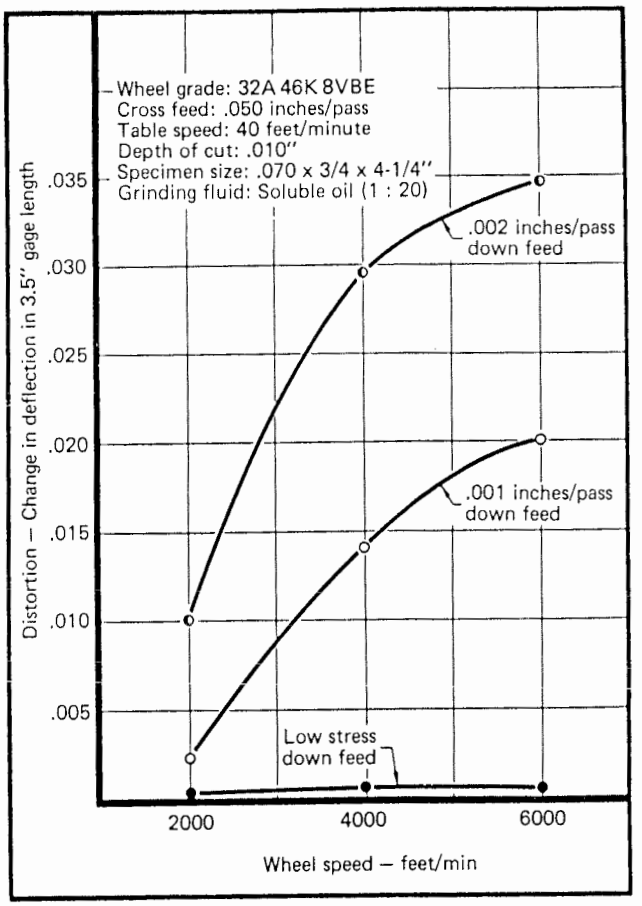

Fig. 11. Change in deflection versus wheel speed for surface grinding; D6 AC steel quenched and tempered to 56 R_c. Effect of down feed.

or

$$\sigma = -\frac{E}{\nu}\left(\frac{d_s - d_u}{d_u}\right) \tag{4}$$

σ = elastic stress
E = Young's Modulus
ε = elastic strain
ν = Poissson's ratio

In order to avoid the need of measuring the interplanar spacing in an unstressed specimen, the two-exposure method may be used. The interplanar spacing of a given set of planes lying at some angle ψ relative to the surface is measured. Such a situation is illustrated schematically in Figure 13 [24]. In the first exposure, the interplanar spacing for planes parallel to the surface is measured by having the incident X-ray beam normal to the surface or at the diffraction angle θ to the surface. The second exposure determines the interplanar spacing for the same set of planes at an angle ψ to the surface. This is obtained by moving the incident X-ray beam to a position which makes an angle ψ relative to the first position. These

TABLE 8

Etching Techniques for Detection of Grinding Injury in Hardened Steel (13)

Operation	Solution Used	Description, Time, or Function
	Double Etch Method	
(1) Etch # 1	4 to 5% Nitric acid in water	Until black, 5 to 10 seconds. Do not over etch.
(2) Rinse	Warm water	To remove acid
(3) Rinse	Methanol (or acetone*)	To remove water
(4) Etch # 2	5 to 10% Hydrochloric acid in methanol (or acetone*)	Until black smut is removed, 5 to 10 seconds
(5) Rinse	Running warm water	To remove acid
(6) Neutralize	2% Sodium carbonate + phenolpthalien indicator in water	To neutralize any remaining acid
(7) Rinse	Methanol	To remove water
(8) Dry	Warm air blast	
(9) Oil dip	Low viscosity mineral oil with rust inhibitor	Enhance contrast, prevent corrosion
	Nital Etch Method	
(1) Etch	5 to 10% Nitric acid in ethanol or methanol	Until contrast is evident

Repeat steps 5-9 above.

Dark areas are overtempered; light areas are rehardened, uniform gray indicates no injury.

* 4% HNO_3 in water for Etch # 1 used with 2% HCl in acetone for Etch # 2 sometimes gives greater sensitivity on high carbon hardened steel. It is important that appropriate precautions be taken to avoid fire hazards and good ventilation must be provided.

conditions are shown in the sketch, AO being the beam normal to the surface to determine the interplanar spacings $d_\perp$, and BO the beam at an angle ψ to the normal for the interplanar spacings d_ψ. Using these values, a stress may be calculated from the following equation:

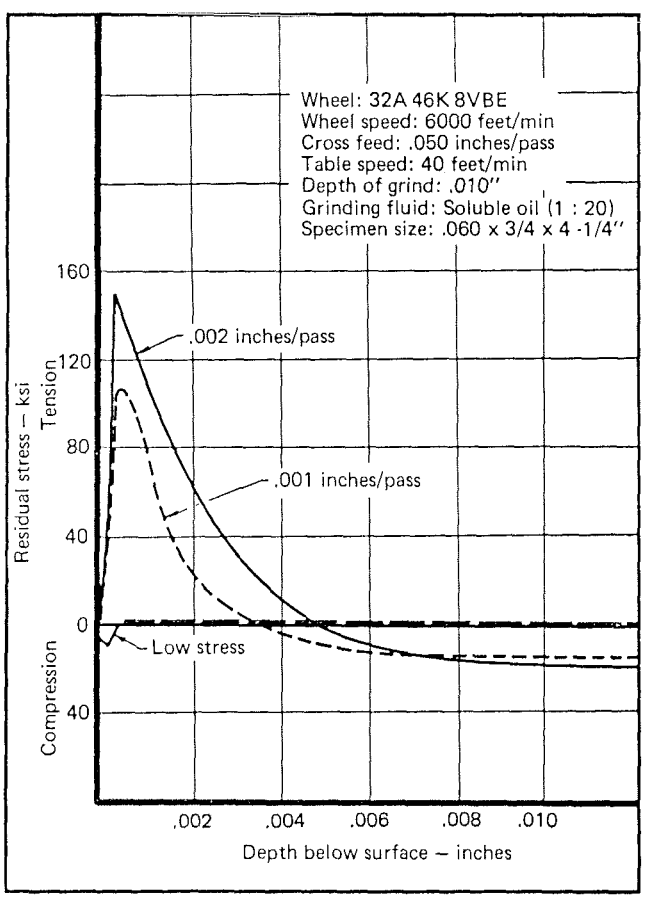

Fig. 12. Residual stress in ground surface; D6 AC steel quenched and tempered to 56 R_c. Effect of down feed.

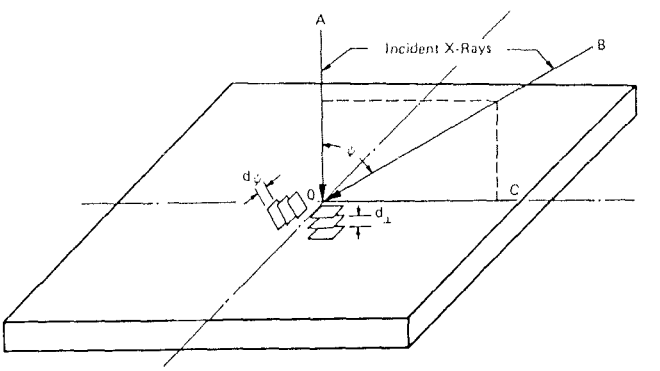

Fig. 13. Schematic of two-exposure X-ray diffraction method [24].

$$\sigma = \frac{E}{(1+\nu)\sin^2\psi}\left(\frac{d_\psi - d_\perp}{d_\perp}\right) \qquad (5)$$

The stress has both magnitude and direction. The direction is determined by the intersection of the plane formed by the two incident X-ray beams and the surface of the metal. This is indicated by OC in Figure 13.

In practice the interplanar distances are not calculated but only the diffraction angles are measured. Therefore, the equation may be modified as follows:

$$\sigma = \left(\frac{E}{1+\nu}\right)\left(\frac{\cot\theta}{\sin^2\psi}\right)\left(\frac{2\theta_\perp - 2\theta_\psi}{2}\right) \qquad (6)$$

E = Young's Modulus

ν = Poisson's ratio

θ = diffraction angle

$\theta_\perp$ = diffraction angle in the normal measurement

θ_ψ = diffraction angle for the inclined angle measurement

ψ = inclined angle

For stress measurements on a given material, the terms not involving the angle θ are constant and Equation (6) can be expressed as:

$$\sigma = K(2\theta_\perp - 2\theta_\psi) \quad (7)$$

where:

$$K = \left(\frac{E}{1+\nu}\right)\left(\frac{1}{\sin^2\psi}\right)\left(\frac{\cot\theta_\perp}{2}\right) \quad (8)$$

The constant K is referred to as the stress factor. Mechanically measured elastic constants are not generally appropriate for calculating the stress factor K. To determine E and ν for X-ray diffraction application, a calibration procedure is obtained directly by shifts in d spacing for a series of applied loads on a calibration specimen [20].

X-ray diffractometers are used to determine the lattice spacing d or peak position 2 θ at the various ψ specimen orientations. With the diffractometer, an X-ray beam of a suitable monochromatic wavelength λ is diffracted off the specimen and the 2 θ shift in the position of a particular high angle diffraction line is determined as a function of the specimen orientation ψ, Figure 14. The accuracy in measurement of residual stresses using X-ray diffraction techniques is dependent on the differences in angle of the diffraction line peak maximum when the sample is examined with its surface at two different angles to the diffracting planes. These diffracting angles must be determined to an accuracy of .01 to .02 degrees. For most surfaces produced by machining, a very broad diffraction peak is generally obtained.

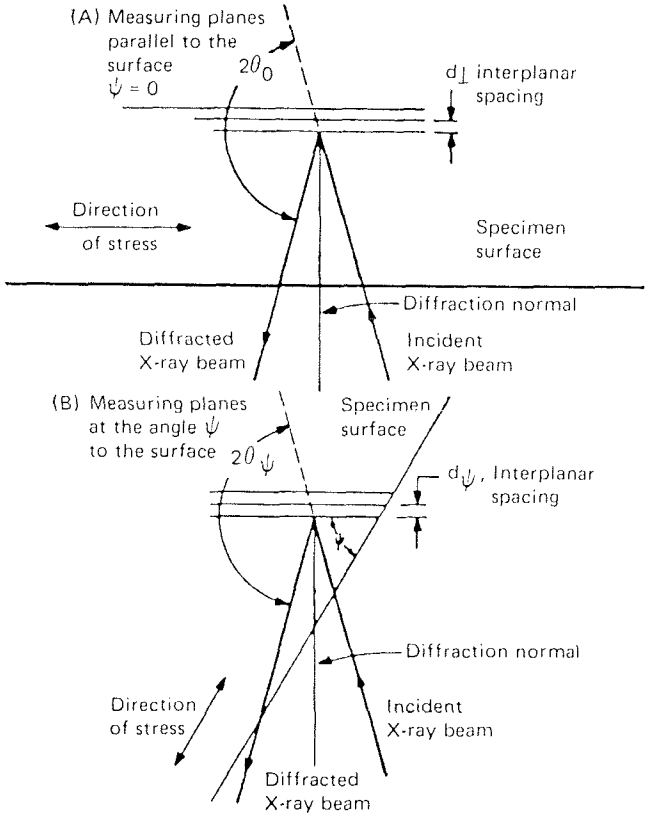

Fig. 14. Schematic showing orientation of measured lattice planes with respect to specimen surface: (A) specimen at $\psi = 0$ exposure, (B) specimen rotated ψ deg [20].

In order to determine the peak location accurately, several methods have been devised [20]. The most popular procedure is to assume that the peak profile follows a parabola. The procedure is to measure only three X-ray intensities within 85 percent of the peak maximum. Experimentally, the diffraction angle range for X-ray intensities within 85 percent of the maximum intensity is established from a chart recording of the peak. Three angles equally spaced are then selected in the immediate vicinity of the peak. The X-ray diffraction intensity is measured at each angle using either preset counts or preset time techniques. Furthermore, the average intensity has to be corrected for Lorentz, polarization and absorption factors. The peak center 2 θ is then calculated by fitting a parabola to the three points. This step is followed first with the specimen normal to the incident specimen ($\psi = 0$) and then with the specimen at an angle ψ, usually 45 degrees, to the incident specimen. The stress is then calculated from Equation (7).

The X-ray technique measures the stress at the surface essentially to a depth of approximately .0002 in. To obtain the stress profile—that is, the stress distribution at various depth below the surface—thin layers must be successively removed and the stress determined after each removal operation. Care must be exercised to avoid introducing additional stresses; normally electrolytic methods are best suited for this purpose. In addition, when the stress layers are removed, the successive measured stresses at depths below the surface must be corrected by an amount related to the relaxation created by the removed layers [20]. This means that all stress determinations by X-ray diffraction, except the initial surface value, must be corrected in order to obtain the true stress which existed when the specimen was intact.

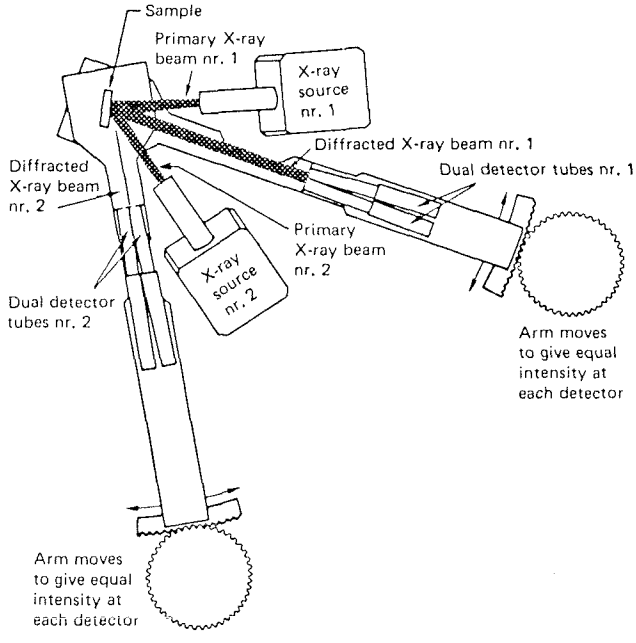

Fig. 15. Sketch showing fastress automatic residual stress analyzer [25].

The determination of residual stress using an X-ray diffractometer is time consuming. To obtain the data necessary for a single residual stress value will require between a half hour to one hour. Recent developments in fast reading X-ray diffractometers have made it possible to determine the residual stress in seconds or in a few minutes. One instrument called Fastress utilizes two X-ray tubes which can measure residual stresses in as little as 20 to 60 seconds [25]. The Fastress unit employs two X-ray sources placed at two different ψ angles which simultaneously irradiate a common area of the sample, Figure 15. The unit also has two sets of detector tubes. The output of each set drives a null-seeking mechanism that locates two points of equal intensity at each peak. Corrections for angle-dependent factors are made electrically so that the outputs of the two detector tubes in a set are proportional to true intensities. At the null point, the true peak position lies midway between the two detector tubes. The potentiometers driven by the gear system at the end of each detectometer indicate the 0 degree and 60 degree (or 45 degree) peak position directly. Because the difference between these voltages is proportional to stress, the recorder is calibrated to read in pounds per square inch. The accuracy in stress determination with this equipment is a function of the time allowed for each stress reading. For example, on a steel sample an accuracy of $\pm$ 10,000 psi was obtained with a determination time of 0.3 minutes. When the determination time was 3 minutes, the mean stress was repeated to an accuracy of $\pm$ 3,000 psi.

Another instrument for the rapid determination of residual stress is a unit called the Simultaneous X-ray Residual Stress Analyzer which can simultaneously produce two X-ray beams [26, 27]. This apparatus, Figure 16, employs an X-ray

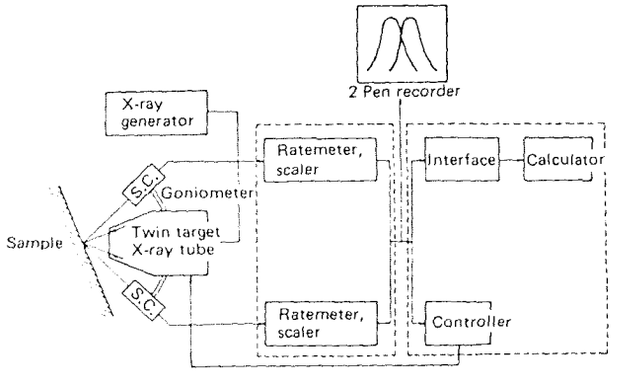

Fig. 16. Block diagram of simultaneous X-ray residual stress [26].

tube having one filament and two targets provided opposite each other on the tube wall. There are two detector systems, a goniometer, and a two-pen recorder system. The X-ray tube includes two targets arranged at an angle of 45 degrees and a filament which bombards them with electrons of uniform intensity, producing two beams of characteristic X-rays simultaneously. The measurement time for determination of residual stress is between one and two minutes.

Both Fastress and the Simultaneous X-Ray Residual Stress Analyzer offer the possibility of studying residual stress in many new applications. For example, these units can be used for quality control of components that have been post-processed by peening to introduce residual compressive stress. Repeated residual stress scanning of peened surfaces is being employed to determine point-by-point residual stress variation over a large surface area. Since residual stress in surfaces can be measured quickly, it will be possible to do more work in stress relaxation and other stress oriented problems.

The X-ray method has certain advantages and disadvantages as a method of determining residual stresses. The advantages are:

a) the stress may be measured in various directions on the surface
b) the stress may be determined in a small area (the exposed area may be less than $^1/_8$ in. in diameter)
c) good accuracy may be expected, $\pm$ 5000 psi
d) it is a rapid method for determining surface stresses
e) it is a nondestructive method for finding the stress *at* the surface
f) the method can be adapted to production parts of various sizes and shapes

The principal disadvantages are:

a) more elaborate and expensive equipment than for the deflection layer-removal method is required
b) since only a small area is exposed for analysis, the stress characteristics may not be indicative of the surface as a whole
c) if the stresses below the surface are required, successive layers must be removed as in the change-in-deflection layer-removal method
d) the accuracy of residual stress measurement is limited in some materials because of the inability to find radiation of suitable wavelength for diffraction from hkl planes close enough to $\theta = 90$ degrees.

2. Layer Removal-Deflection Technique

This method uses the change in deflection resulting from the removal of successive layers from the machined surface of the test specimen previously described to calculate the residual stress. The removal of a stressed layer produces a rebalancing of the stresses across the section and a change in deflection of the specimen.

Stäblein [28] presents two equations for calculating the unaxial stress; the one for the case when the specimen is held in the flat position (Equation 9) and the other for the case when the specimen is free to bow (Equation 10).

$$\bar{\bar{\sigma}} = \frac{E\delta^2}{6}\left|\frac{dk(\delta)}{d\delta}\right| + \frac{2E}{3}\delta k(\delta) - \frac{E}{3}\int_{\delta}^{d} k(\delta)\,d\delta - \frac{Ed}{6}k(d) \quad (9)$$

$$\sigma = \frac{E}{6}\delta^2\left|\frac{dk(\delta)}{d(\delta)}\right| + \frac{2}{3}E\delta\left|k(\delta) - k(d)\right| + \left(\frac{d-\delta}{3}\right)Ek(d) - \frac{E}{3}\int_{\delta}^{d} k(\delta)\,d\delta \quad (10)$$

$\bar{\bar{\sigma}}$ = stress in the longitudinal direction when the specimen is clamped flat after etching to thickness δ

σ = stress in the longitudinal direction when the specimen is free to bow after etching to thickness δ

E = Young's Modulus of Elasticity

δ = thickness of the specimen after each incremental layer is removed

$k(\delta)$ = curvature of the specimen after incremental layers are removed to thickness δ

d = thickness of the specimen before incremental removal of stressed layers

k (d) = curvature of specimen before incremental removal of stressed layers

$\frac{dk(\delta)}{d(\delta)}$ = slope of the curvature vs. thickness curve at the etched thickness

The normal procedure is to measure the radius of curvature in terms of the deflection over a given gage length. If L = $^1/_2$ gage length, f = deflection, and r = radius of the curvature, then

$$r = \frac{L^2}{2f} \quad (11)$$

In reference 29, this substitution was made to give the equations in the form:

$$\bar{\bar{\sigma}} = \frac{E}{3L^2}\left[\delta^2\left(\frac{df}{d\delta}\right) + 4\,\delta f - df_o - 2\int_{\delta}^{d} f\,d\delta\right] \quad (12)$$

$$\sigma = \frac{E}{3L^2}\left[\delta^2\left(\frac{df}{d\delta}\right) + 4\delta(f-f_o) + 2f_o(d-\delta) - 2\int_{\delta}^{d} f\,d\delta\right] \quad (13)$$

where the additional terms not defined in connection with Equations (9) and (10) are:

L = one half the span or gage length used for the deflection measurements

f_o = midspan deflection before incremental removal of stressed layers

f = midspan deflection after each incremental layer is removed

$\left(\frac{df}{d\delta}\right)$ = slope of the deflection vs. thickness curve at the etched thickness

Note: The sign of the deflection is positive (+) when the test surface is concave, negative (−) when the test surface is convex.

As will be noted in the above equations, the original thickness, the original deflection, the deflection associated with a given etched thickness and the slope of the deflection vs. thickness curve at that etched thickness, $(df/d\delta)$, are required. Since experimental data are subject to some degree of variation, the deflection vs. thickness data are plotted and a smooth curve drawn through the experimental points. From such a curve appropriate points are selected for slope determinations. When there is a rapidly changing slope, the thickness interval between slope determinations should be kept small. A typical deflection vs. thickness curve is shown in Figure 17.

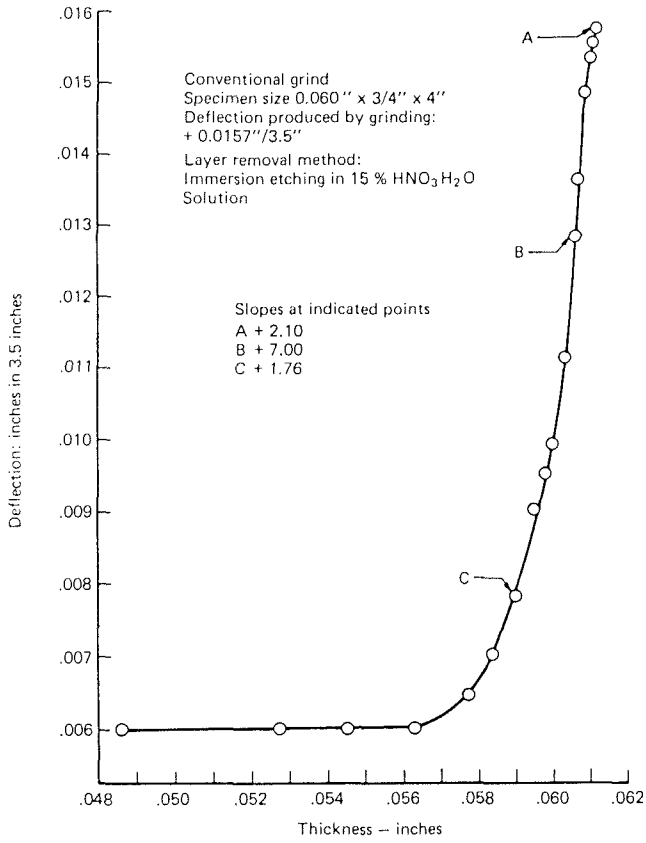

Fig. 17. Deflection VS. Thickness curve for AISI 4340 steel, 50 R_C.

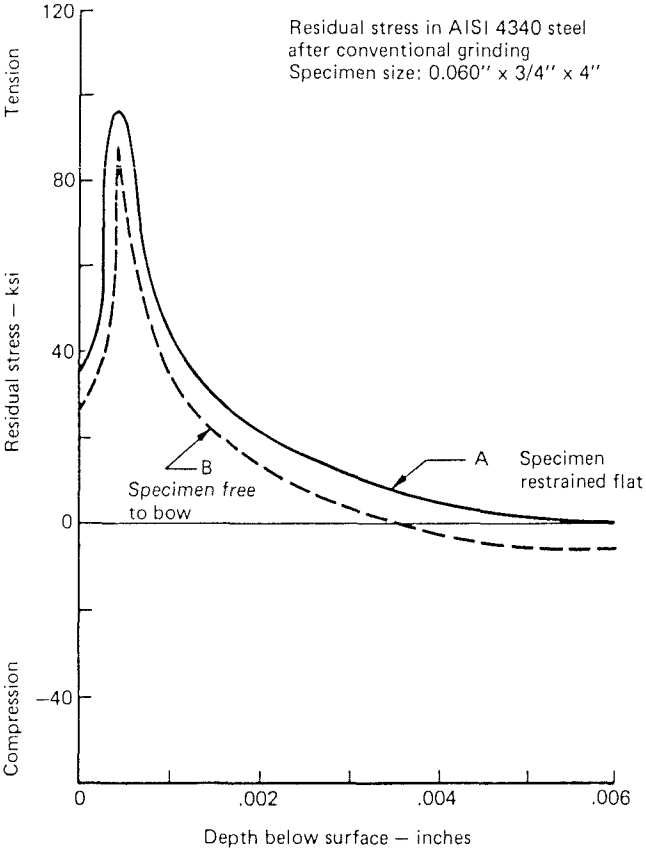

Fig. 18.

It will also be noted from the equations that the calculated stress value is strongly dependent on the magnitude of the slope of the deflection curve. For a given machining test condition, a greater deflection will be obtained with a thinner test specimen, however, the effect of the method used to measure the deflection must be considered. If a dial indicator is used, the spring tension of the indicator prohibits the use of very thin specimens. Increased sensitivity may be obtained by using an optical interference or a linear variable differential transformer method for determining the arc height.

In Figure 18, the calculated stress values used to plot the residual stress curves shown were obtained from Equations (12) and (13) and the deflection curve in Figure 17. Curve A shows the stress distirbution when the specimen is restrained in the flat position, while Curve B shows the stress distribution when the specimen is free to bow after test machining. It will be noted that in this particular test the maximum stress was not found at the surface, but at approximately .0005 in. below the surface.

Both the X-ray diffraction and the change-in-deflection, layer-removal methods require the successive removal of incremental layers from the machined surface in order to find the residual stress profile. However, the change-in-deflection, layer-removal method has the decided advantage of using relatively simple and inexpensive equipment for the obtaining of reliable residual stress data.

Biaxial surface stresses can also be determined by a layer removal-deflection technique. Letner employed a 2 in. × 2 in. × .200 in. specimen [30]. He measured the surface stress in two perpendicular directions parallel to the two sides of the specimen and employed Stâblein's equations to calculate the residual stress. In order to obtain the residual stress, it was necessary to measure the deflection in the two perpendicular directions. This was done by using an accurate electrical comparator.

Decneut and Peters have developed a layer removal technique which continuously etches away, calculates and computes the residual stress pattern in the specimen [31]. The residual grinding stresses on ball bearing rings were measured in the grinding direction by Decneut and Peters using this deflection method. Thin layers were removed from the ground surface by continuous electrolytic etching, and the residual stresses present in the etched-off layers were calculated from the change in deflection of the workpiece. The procedure is fully automatic, yielding a high rate of data output which is recorded on punched tape for subsequent computer treatment.

C. Static Properties

1. Tensile and Creep Rupture Testing

Important static properties of interest which may possibly be affected by the method of machining are tensile and creep rupture behavior. It has generally been found that only the very severe surface alterations, such as extreme surface roughness or cracking, have an appreciable effect on static properties. One interesting exception, however, has been a notable decrease in ductility and tensile strength on materials that have been processed by electrical discharge machining (EDM) followed by a stress relief heat treatment [32]. It was found that a carbon deposit produced on the surface during the EDM operation was diffused into the grain boundaries during a subsequent stress relief heat treatment and caused an excessive grain boundary precipitation of carbides. These precipitates were responsible for reductions in ductility and strength, the extent of which was found to be a function of the surface roughness, see Figure 19. Reductions in tensile ductility as high as 80 percent were noted after heat treatment in the testing of specimens of Inconel 718 which had been EDM'd to a surface finish of 650 RMS.

The technique recommended for determination of tensile properties including ductility is the use of a standard ASTM round or flat specimen [33]. Specimens from ¼ in. to ½ in. in diameter or width with a gage length four times this dimension are suitable. The standard technique usually calls for a strain rate of .005 in./in./min. until the yield point is passed and then an increased overall loading rate of .05 in./min. to fracture. The load strain curve is normally recorded, permitting the calculation of ultimate tensile and yield strengths. Ductility is measured in terms of percent elongation and/or reduction of area.

The techniques for creep rupture testing also follow a standard ASTM procedure [34], employing either round or flat specimens. If creep deformation is to be measured, the elonga-

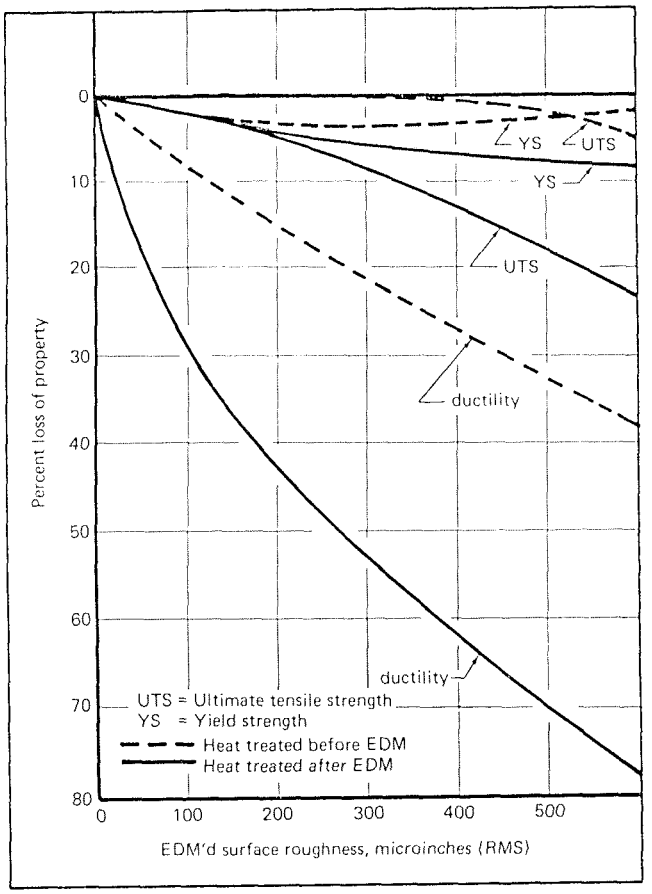

Fig. 19. Property loss VS. Surface finish, alloy 718.

tion can be determined by optical means using a platinum extensometer attached to the specimen and viewed through a window in the furnace. An alternate method of measuring creep is to employ a mechanical extensometer attached to the specimen. The extensometer movement is detected by a linear differential transformer whose output is continuously plotted on a recorder.

2. Stress Corrosion Evaluation

Stress corrosion is a phenomenon which produces failure originating at the surface, and hence the surface character should have a major influence on stress corrosion susceptibility. Stress corrosion susceptibility is difficult to assess; however, it appears to be more prevalent in the presence of certain specific environments when the surface is in tension. It has been found, for example, that the presence of untempered or overtempered martensite in a high strength steel can seriously reduce the time for failure by stress corrosion. Stress corrosion susceptibility increases with increasing hardness and strength of steels. It can also be a serious problem in the application of aluminum alloys, although certain types of aluminum alloys are more resistant to stress corrosion attack than others. Titanium alloys have been found to be especially sensitive to stress corrosion and, in particular, to salt and other halogens when combined with high tensile stresses and temperatures over 500° F.

One of the simple methods of determining stress corrosion susceptibility in steels and aluminum is to prepare a strip specimen such as that shown in Figure 20. This test specimen

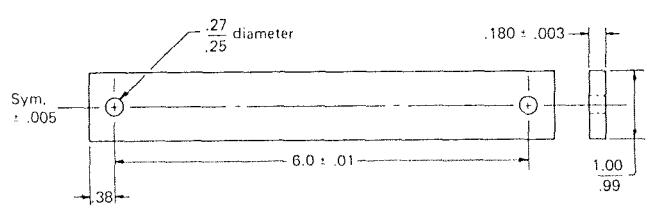

Fig. 20. Stress corrosion specimen.

is then placed in a fixture and bent to produce a surface stress on the test surface to 75-90 percent of the tensile yield strength. The specimen is then mounted singly or in multiples in a test rig which submerges the bent specimen in a solution of sodium chloride and then withdraws it into air. One such device consists of a large rotating drum which carries a series of specimens. The drum slowly revolves so that the specimens are dipped and immersed in a tank of 3 to 4 percent sodium chloride for 10 minutes and then brought into air, remaining there for a period of 50 minutes. The specimens are examined periodically until a crack is observed by visual observation using a low power magnifying glass. In still other stress corrosion tests on steel and aluminum, specimens are mounted singly or in multiples in a stress rupture machine under constant load. The specimens are surrounded by a suitable container to which a salt solution is alternately added and emptied according to a prescribed time schedule. The specimens are observed periodically for cracks.

Stress corrosion tests described above are usually devised so that failures occur under 1000 hours. Additional stress corrosion tests have been developed covering a period of years. For example, one series of tests consisted of evaluating the effect of methods of producing holes in high strength steel bars. The bars containing the holes were then loaded in fixtures which applied a predetermined stress. The fixtures containing the stressed specimens were placed in a seacoast environment. It was found that bars containing holes which were drilled so as to form untempered or overtempered martensite produced failure within six months whereas holes that were honed to remove all traces of untempered and overtempered martensite did not fail after a period of five years.

An intensive effort has been performed on titanium alloys which appear to be especially susceptible to stress corrosion cracking when halides are present, particularly sodium chloride even in minute quantities. Extreme depressions in stress corrosion life have been found when titanium alloys are subjected to high stress and high temperatures [35]. Stress corrosion values for titanium alloys have been reduced from thousands of hours to less than 100 hours as a result of a combination of salt, high stress, and high temperature. Stress corrosion cracking can occur when a chlorinated fluid is present on sheet titanium materials heated to elevated temperatures during a press-bending operation. Thus, when chlorinated cutting fluids are not properly washed off sheet titanium which is heated to 1000° F and placed in a press-brake, cracks will generally occur.

3. Fracture Toughness Testing

In the realm of surface integrity, fracture toughness considerations are seldom involved since fracture toughness relates to growth of a fatigue crack once it is present, whereas surface integrity effects usually are associated with fatigue crack initiation. In certain situations, where potentially corrosive environments resulting from manufacturing operations persist, fracture toughness may, however, become a part of a surface integrity situation. In the drilling or milling of an assembly, for example, it may be impractical to remove all of the cutting fluid from the area involved. Should cracking develop, contamination from the cutting fluid could possibly affect fracture toughness of the material and hence component performance.

Fracture toughness tests have been developed to provide a quantitative means of measuring the inherent resistance of a material to sudden or unstable crack growth under static loads. A variety of test techniques have been proposed in recent years. Several of these have proved to be effective and are being used in various segments of industry. Two of the more commonly used test specimens, the precracked beam and the compact tension specimen, are covered by a recent ASTM standard, E399 [36]. A compact tension specimen of a typically employed size is shown in Figure 21. The fracture toughness test involves determination of the critical crack tip stress intensity factor which initiates unstable crack growth. The stress intensity factor relates the applied stress, crack size, and configuration of the load-crack system. A general equation for the stress intensity factor is as follows:

$$K = \sigma a^{\frac{1}{2}} \times f$$

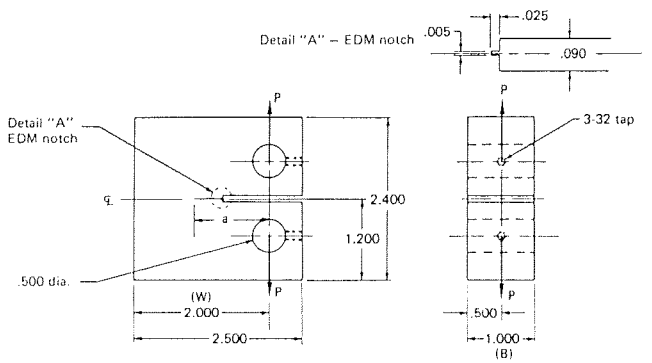

Fig. 21. Compact tension specimen.

where:

σ = applied nominal stress
a = crack length
f = function accounting for configuration of the load-crack system

Specifically, for the compact tension specimen mentioned above and shown in Figure 21:

$$K = \frac{P}{BW}(a)^{\frac{1}{2}}\left[29.6\text{-}185.5\left(\frac{a}{W}\right) + 655.7\left(\frac{a}{W}\right)^2 - 1017\left(\frac{a}{W}\right)^3 + 638.9\left(\frac{a}{W}\right)^4\right]$$

where: P = normal load applied to specimen, pounds
B = thickness of specimen, inches
W = length of specimen, inches

While stress intensity at the crack tip K is a function of all of the factors involved, the critical stress intensity at which unstable crack growth will occur (hence catastrophic failure) is an inherent property of a material. This critical stress intensity factor, under plane strain conditions, is called K_{Ic}.

Fracture toughness data, K_{Ic}, are widely employed in the design of critical components. The data are useful in material selection, material quality control, establishment of critical crack sizes for given operating stress levels, and establishment of nondestructive testing sensitivity requirements to avoid catastrophic failures. To evaluate surface integrity situations where continual exposure to residual cutting fluid may result in embrittlement or otherwise altered fracture toughness, the K_{Ic} value obtained by testing in such environments is labeled as being altered by the test environment. In evaluating the effect of saltwater immersion, for example, fracture toughness values are referred to as K_{salt} measurements. The effective presence of an aggressive environment is indicated by the numerical lowering of a K_{Ic} level.

D. Dynamic Properties

High cycle and low cycle fatigue are two important dynamic properties which are surface dependent. High cycle fatigue is probably the more important of the two and likely the most important mechanical property affected by the surface condition produced during machining or other processing. Low cycle fatigue strength is also affected by processing but to a smaller degree. In fact, if the low cycle fatigue testing is accomplished at a very low frequency and very high stress, the low cycle fatigue strength approaches the static strength of various materials.

1. High Cycle Fatigue Determination

The effect of the surface condition can best be evaluated by employing an alternating stress with a zero mean stress. A specimen which has been found to be extremely useful is a cantilever bending specimen shown in Figure 22. This specimen has a tapered section which provides uniform stress over the length of the taper. This specimen is gripped at one end and vibrated at the small end with a uniform force or at constant amplitude, Figure 23. A flat specimen is particularly useful in that a variety of machining operations similar to those used in actual shop processing can be performed on each side of the specimen. When testing such a specimen, there is always a tendency for the specimen to fail at the edge rather than in the face of the test surface. To prevent edge failure, the specimen edges are carefully radiused, then polished and shot peened, see Figure 22. A template mask is placed over the flat test surfaces so that the shot peening is restricted to the edges. Generally, it is also necessary to shot peen the flat grip area to prevent contact fatigue failure during testing. Tests are usually run at zero mean stress until failure occurs; when failure does not occur, tests are usually terminated at 10^7 cycles. A stress versus number of cycles (S/N curve) can be plotted, and from this plot the endurance limit is determined, Figure 24. The endurance limit is defined as the stress below which no

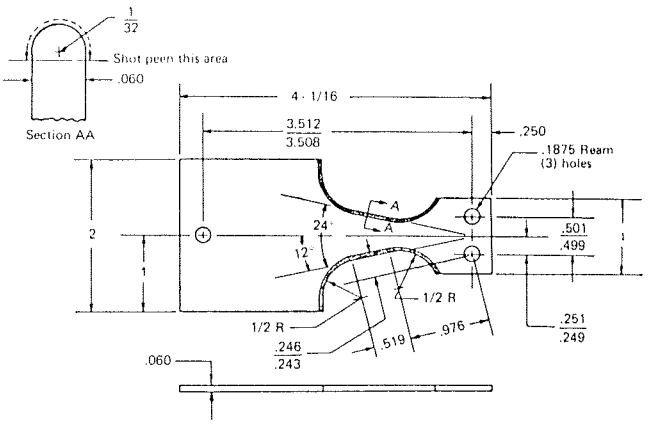

Fig. 22. High cycle fatigue specimen. Grinding and milling.

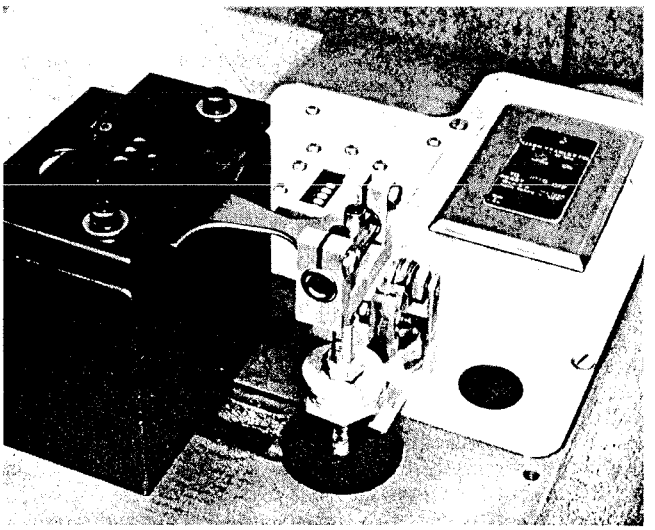

Fig. 23. High cycle fatigue setup.

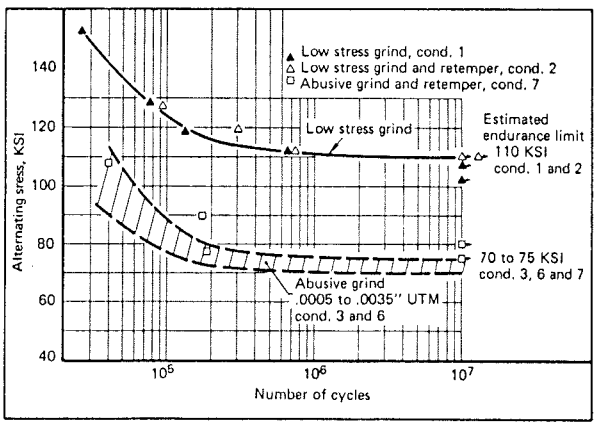

Fig. 24. Low cycle fatigue specimen, grinding and milling.

failures will occur up to the runout value of 10^7 cycles. This test can be performed at room or elevated temperatures. Heating for elevated temperatures can be accomplished either by induction heating or by resistance heating. In induction heating, an induction coil is placed around the test section; in resistance heating, a resistance coil is placed around the test specimen. In both methods, suitable precautions have to be taken to prevent overheating of the grip and vibratory ends of the specimen.

Additional fatigue testing procedures which have been employed include axial loading of round or flat specimens and rotating beam testing of round specimens. In addition, larger specimens are frequently employed by design engineers in order to simulate more closely the design parameters of actual component evaluation. However, these procedures are suggested primarily for more sophisticated evaluation of surface effects when more exact design data are required for important hardware components.

2. Low Cycle Fatigue Determination

A four-point bending specimen has been chosen for low cycle fatigue testing for three reasons [37]. First, the bending condition is similar to the high cycle fatigue condition. Second, this specimen design provides for a large surface area under uniform stress. Third, the circular displacement curve of the specimen under load allows direct determination of surface strain at elevated temperatures using a spherometer.

The specimen selected, Figure 25, allows a nominal gage section surface area of two square inches. The edges of the reduced cross section are rounded, polished, and shot peened to reduce the chance of edge failure.

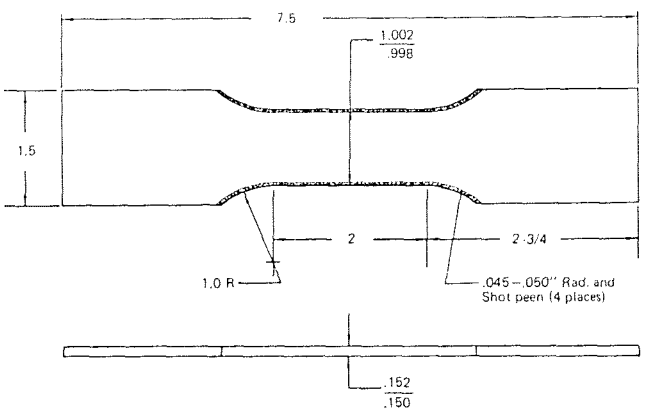

Fig. 25. Low cycle fatigue setup.

Low cycle fatigue tests are conducted on a closed-loop servo hydraulic machine designed and built at Metcut Research Associates Inc. The design is basically the same as that of commercially available closed-loop testing machines. The four-point bending fixture, as shown in Figure 26, is attached directly to the hydraulic ram. The tests are conducted in fully reversed bending with controlled fixture amplitude, and a triangular displacement waveform is generally used at frequencies from 10 to 30 cpm.

Within the strain range employed in this test, the specimen surface strain is directly proportional to the fixture displacement. This has been found to be true for a wide range of materials and stress levels. The relation between strain and fixture displacement is fundamental to the test technique and has been verified with resistance strain gages at room temperature and spherometer measurements at elevated temperatures. Elevated temperature tests are conducted using induction, radiant or direct resistance heating techniques. With radiant or induction techniques, a one inch center zone of the gage section can be maintained within $\pm 10^\circ$ F of the desired test temperature.

The data of primary interest are the maximum surface strain amplitude, the specimen dimensions, and the number of cycles to failure, N_f. For stress levels beyond the proportional limit of the test material, data are reported in terms of pseudo stress. Pseudo stress is taken to be the product of the elastic modulus and the maximum strain. Typical test data comparing abusive and gentle surface grinding conditions are shown in Figure 27 [37].

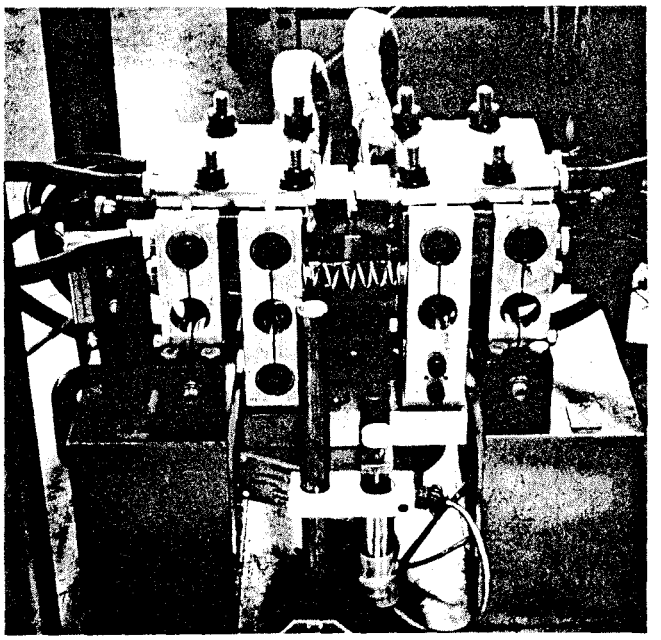

Fig. 26.

3. Fatigue Crack Propagation

Consideration should also be given to fatigue crack propagation testing which is carried out to determine the relative resistance of materials to the growth of fatigue cracks. The specimens normally used are of several varieties having the capability of promoting uniform crack growth characteristics under repeated cyclic loading. Compact tension specimens such as used for fracture toughness testing, Figure 21, and also center notched panels such as used for studying the toughness of sheet are perhaps the two most common specimen varieties used in fatigue crack propagation testing. Testing is usually performed in the tension-tension or tension-zero-tension mode using either mechanical, hydraulic or electromagnetic fatigue equipment. Testing techniques involve the repeated measurement of fatigue crack growth as a function of the number of loading cycles. Optical techniques are most frequently used for measuring the extent of fatigue crack growth, although ultrasonic and other sophisticated techniques are sometimes employed.

From the specimen geometry and loading, the stress intensity factor present at the tip of the crack can be defined mathematically using techniques of linear elastic fracture mechanics [38, 39]. The rate of fatigue crack growth is measured as a function of the cyclic stress intensity factor range. A typical

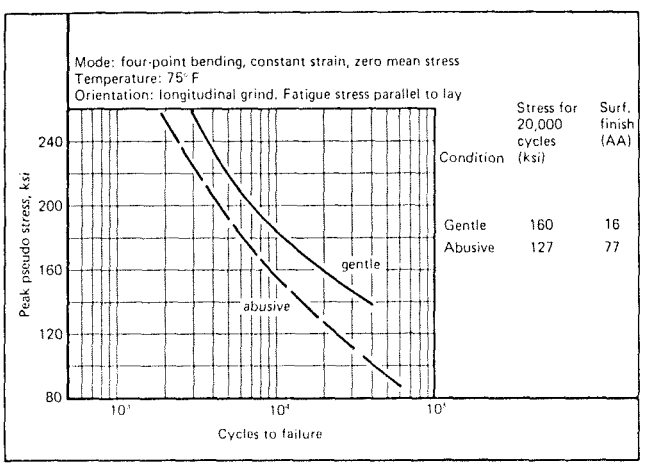

Fig. 27. Low cycle fatigue characteristics of inconel 718 (solution treated and aged, 44 R_c) produced by surface grinding.

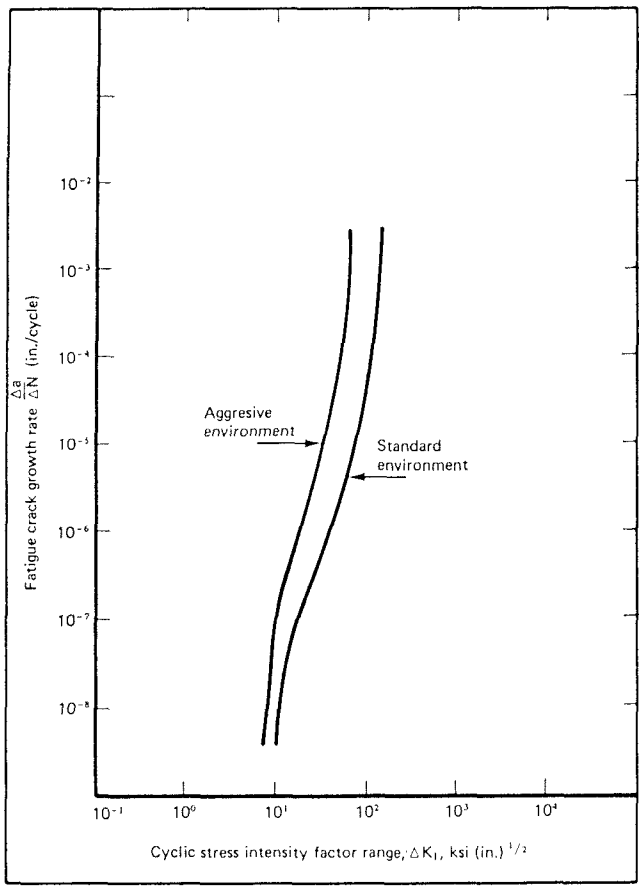

Fig. 28. Schematic representation of fatigue crack growth rate curves.

crack propagation rate curve is shown in Figure 28. Comparisons of the crack propagation resistance of various materials as well as various heat treated conditions for a single alloy are usually made at the same stress intensity level. The evaluation of fatigue crack propagation rates can be carried out under almost any environmental conditions of interest. For example, testing can be performed over the range of temperatures of interest for a particular material. It is likewise possible to perform such tests in air, in vacuum, or under an almost limitless variety of corrosive conditions as may be applicable.

Like fracture toughness testing, fatigue crack propagation testing will in some instances have a peripheral relationship to surface integrity. In situations where surface contamination due to cutting fluids or other environmental factors is present in the vicinity of a growing fatigue crack, these surface integrity factors may affect the crack growth rate of the material. The type of situation in which this can occur is as previously discussed in the section on Fracture Toughness. Where a contaminating environment is aggressive or detrimental to crack growth resistance, the fatigue propagation rate curve, as shown in Figure 28, is shifted to the left, indicating an increase in growth rate. The more aggressive the environment, the further to the left will be the displacement of the curve.

There are three distinct advantages related to crack propagation testing with utilization of fracture mechanics analysis:

a) The data permit a direct evaluation of the influence of various environments on crack growth rate. Aggressive environments can be identified readily.

b) The data are the basis for fatigue life analysis in terms of propagation of defects which may be inherent in the material or introduced in component manufacture.

c) These data and the appropriate analysis may be applied directly to determine the expected fatigue life of structural components under comparable environmental conditions in service.

Analysis of Surface Chemistry

During the past few years, several new techniques have been developed for chemically analyzing engineering surfaces. Commercial instrumentation is now available which is capable of characterizing solid surfaces down to depths of about one micron. These methods include: ion scattering spectometry, Auger electron spectroscopy, electron spectroscopy for chemical analysis (ESCA), and ion probe mass spectrometry, listed in increasing order of depth from which they can generate analytical information [40].

Since the newer analytical techniques can sample as little as one monolayer of material or proceed up to sampling several tens of microns in depth, it is important to define the depth from which a surface analysis is required in an engineering material before identifying the particular type of instrument that should be utilized.

Ion scattering spectrometry utilizes inert gas ion bombardment of a surface, and by determining the energy changes produced in this beam as it scatters off target atoms on the surface, the technique can identify the elements present in a monolayer of material [40]. Elements of atomic number 3 (Li) and up can be detected, although to get complete coverage across the periodic chart requires using several different inert gas ions in sequence because target atoms which differ too greatly in mass from the primary ions are difficult to distinguish from one another. Within the region bombarded, information on the spatial distribution of the constituents cannot be obtained. By continued sputtering in a region, it is possible to obtain data on composition changes with depth, reaching 10-20 monolayers in reasonable lengths of time (hours).

A composition depth profile analysis of Rene' 41 is shown in Figure 29 [41]. This profile was accomplished by the dual utilization of the probe ion beam for both detection and identification of the surface atoms and also for the controlled removal of surface monolayers through sputtering. Rene' 41 is a nickel base alloy containing about 50 percent by weight of nickel. The surface was found to be depleted of nickel to a depth of about 10 monolayers. In fact, the bulk composition does not appear until a depth of 50 monolayers has been reached.

Auger electron spectroscopy involves a nondestructive analysis based on the ejection of low energy Auger electrons from a surface under electron bombardment [40, 42]. The analytical information is obtained from a penetration 5-10 Å into the sample. Two dimensional microcompositional data from the material are not produced, but by use of an associated ion gun, depth profiles can be determined over many hundreds of angstroms in depth. Elements above Li can be detected, and

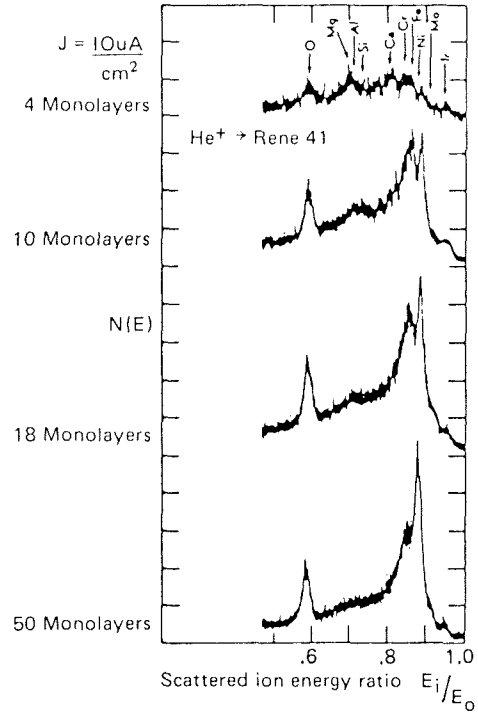

Fig. 29. Composition depth-profile of a Rene'41 surface obtained by a time sequential series of partial ion scattering spectra utilizing 1500eV He+. The apparent surface depletion of Ni is shown [41].

a major advantage is the ability to analyze highly topographic surfaces like fracture faces.

ESCA also utilizes an electron bombardment but detects instead the ejection of higher energy inner shell electrons [40, 43]. Consequently, it derives its information from a depth of 30-50 Å in the sample. Its analytical capabilities are somewhat similar to Auger spectroscopy, although ESCA appears to have a distinct advantage in determining "chemical shifts" in the ejected electrons which can reveal significant aspects of the chemical state (bonds) on the surface.

Ion probe mass spectroscopy employs layer-by-layer ion bombardment of a sample using 0_2^+, $A+$, etc., and is readily capable of carrying out a surface analysis to depths in excess of several microns [40, 44]. Moreover, elements from hydrogen to uranium can be detected, and both two and three dimensional microcompositional data can be obtained. The sputtering of material from the sample generates a variety of positive and negative ions which reflect the composition and chemical associations on the surface. While the state of the art can identify such associations semiquantitatively, the complete determination of surface compounds based on secondary ion production remains to be established.

Conclusions

Recognition and application of surface integrity technology are increasing as evidenced by the widespread interest in the subject and by the adoption and use of detailed surface integrity specifications for purchasing and manufacturing of critical components. Consequently, increased pressure is being exerted to properly assess a surface integrity situation and to measure and control surface conditions which may impair or enhance surface quality.

At the present time, there are many simple techniques for measuring surface integrity which when properly applied are extremely useful in improving the structural integrity of components under service conditions. These have been summarized in this paper as the *Minimum Surface Integrity Data Set*. With regard to the application of techniques such as microscopy, microhardness testing, and even the more sophisticated tests, it is of paramount importance to isolate and to define properly the specific surface integrity problem in question. Then, particular test methods, many of which are already well established and accepted, may be specified to control the manufacturing processes in question.

With regard to manufacturing processes, there has been a reluctance on the part of engineers and managers to rely upon in-process control. However, in view of the general lack of adequate nondestructive testing equipment for final inspection, there are often no alternatives. Our experience has shown that once the seriousness of a surface integrity situation is recognized, it is possible to set up shop procedures to achieve control. In any event, it is important not to go through the motions of using nondestructive test methods which are not capable of recognizing surface integrity problems. For example, we know of no practical testing device which can sense an alloy's propensity to delayed cracking as a result of grinding. Also, we know of no final inspection technique capable of recognizing, under production conditions, patches of recast layer produced by thermal material removal processes which develop deleterious surface layers as thin as .0001 in. Yet, for both of the situations noted above, it was possible to specify and control manufacturing practices so as to avoid failures which had occurred in service.

In summary, if the technology of the production of high quality surfaces is to be advanced further, several important needs must be met. Greatly increased effort must be expended in developing data which relate the physical and chemical condition of surfaces to the significant mechanical properties of components in service. Urgent need also exists for the development of technology and equipment for the nondestructive testing of large and intricate surfaces. Meeting of the above needs and sharing of the information to avoid unnecessary duplication of programs will do much toward increasing the reliability and safety of all types of hardware systems which have a high degree of commonality in domestic and international manufacturing and use.

Refernces

1. Michael Field and J. F. Kahles, 1971. Review of surface integrity of machined components. Annals of the CIRP 20(2): 153-163.
2. D. J. Whitehouse, 1972. Modern methods of assessing the quality and function of surface texture. Paper No. IQ72-206. Dearborn, Michigan: Society of Manufacturing Engineers.
3. J. B. P. Williamson, 1968. Physical aspects of a surface. Paper No. EM68-513. Dearborn, Michigan: American Society of Tool and Manufacturing Engineers.
4. H. T. McAdams and P. A. Reese, July 1970. Surface topography and metal fatigue (Project STOP). CAL report No. KB-2952-D-1. Final report. Buffalo, New York: Cornell Aeronautical Laboratory, Inc.
5. J. F. Kahles and Michael Field, 1971. Surface integrity guidelines for machining, 1971. Paper No. IQ71-240. Dearborn, Michigan: Society of Manufacturing Engineers.
6. L. R. Gatto and T. D. DiLullo, 1971. Metallographic techniques for determining surface alterations in machining. Paper No. IQ71-225. Dearborn, Michigan: Society of Manufacturing Engineers.
7. S. Ramalingam and J. T. Black, 1969. Surface quality evaluation of fabricated components using electron microscopy. In American Society for Nondestructive Testing and Southwest Research Institute, *Symposium on nondestructive evaluation of components and materials in aerospace weapon systems and nuclear applications, 7th, San Antonio, Texas, April* 23-25, 1969, *Proceedings*, pp. 157-164. North Hollywood, California: Western Periodicals Company.
8. Frithjof Betz, "Untersuchungen zur Entstehung der Schnittflächenrauheit bei der spanenden Bearbeitung". Ph. D. Dissertation, Eidgenössische Technische Hochschule Zürich, 1971.
9. Guy Bellows, Aircraft Engine Group, General Electric Company, Evendale Plant, Cincinnati, Ohio.
10. J. T. Black and S. Ramalingam, 1970. Fine structure of machined surfaces. International Journal of Machine Tool Design and Research 10(4): 439-463.
11. Michael Field, W. P. Koster, J. B. Kohls et al., 1970. Machining of high strength steels with emphasis on surface integrity. AFMDC 70-1. Cincinnati, Ohio: Air Force Machinability Data Center.
12. L. P. Tarasov, 1946. Detection causes and prevention of injury in ground surfaces. Transactions American Society for Metals 36: 389-439.
13. W. E. Littman, 1967. The influence of grinding on workpiece technology. Paper No. MR67-593. Dearborn, Michigan: Amercian Society of Tool and Manufacturing Engineers.
14. R. C. McMaster and G. H. Smith, 1967. Principles of the magnetic reaction analyzer—a new eddy current test system. Materials Evaluation 25(7): 153-163.
15. G. H. Smith and R. C. McMaster, 1967. Current aerospace applications using MRA eddy current test systems. Materials Evaluation 25(12): 283-288.
16. S. J. Klima and J. C. Freche, Sept. 1968. Ultrasonic detection and measurement of fatigue cracks in notched specimens. NASA TN D-4782. Washington, D.C.: National Aeronautics and Space Administration.
17. S. J. Klima, D.C. Lesco and J. C. Freche, 1966. Application of ultrasonics to detection of fatigue cracks. Experimental Mechanics 6(3): 154-161.
18. Nondestructive testing: trends and techniques, 1967. NASA SP-5082. Washington, D.C.: National Aeronautics and Space Administration.
19. Ultrasonic tests expose hidden fatigue stress. 1968. Steel 163(1): 46-47.
20. Society of Automotive Engineers, Inc., 1971. Residual stress measurement by x-ray diffraction. SAE J784a. New York, New York.
21. J. R. Zurbrick, February 1969. Development of nondestructive tests for predicting elastic properties and component volume fractions in reinforced plastic composite materials. AFML-TR-68-233. Wilmington, Massachusetts: Avco Corporation, Avco Government Products Group.

22. Rudi Schroeer, November 1968. Research on exploratory development of nondestructive methods for crack detection. AFML-TR-67-167. Part II. Dayton, Ohio: Arvin Systems Inc.
23. W. C. Eddy, Jr., 1969. Radioactive gas penetrant inspections. Columbus, Ohio: Federal Systems Division,Industrial Nucleonics Corporation.
24. F. W. Westermann, 1971. Determining the distortion and residual stresses produced by metal removal operations. Paper No. IQ71-224. Dearborn, Michigan: Society of Manufacturing Engineers.
25. E. W. Weinman, J. E. Hunter and D. D. McCormack, 1969. Determining residual stresses rapidly. Metal Progress 96(1): 88-90.
26. J. Sekita, K. Ogiso, U. Kaminaga et al., 1971. New x-ray apparatus for stress measurement using a calculator. In x-ray study on strength and deformation of metals, seminar proceedings August 23-24, 1971, pp. 81-88. Tokyo, Japan: Society of Materials Science.
27. Yoshihiro N. D. Shimura. Simultaneous x-ray residual stress analyzer using an x-ray tube with single filament and twin target (45° apart). Tokyo, Japan: Rigaku Denki Company, Ltd.
28. F. Stablein, 1931. Spannungsmessungen an einseitig abgelöschten Knûppeln. Kruppsche Monatshefte 12: 93-99.
29. R. J. Kroll, F. E. Westermann and J. K. Cuddeback, August 19, 1970. Expansion of derivation of Stablein's equation for calculating residual stress in a machined surface. Cincinnati, Ohio: Metcut Research Associates Inc.
30. H. R. Letner and H. J. Snyder, July 1953. Grinding and lapping stresses in manganese oil-hardening tool steel. Transactions American Society of Mechanical Engineers 75: 873-882.
31. A. Decneut and J. Peters. Residual stress measurements employing deflection-etching techniques. (To be presented at the International Conference on Surface Technology, Pittsburgh, Pennsylvania, May 1973, sponsored by the Society of Manufacturing Engineers).
32. A. R. Werner and P. C. Olson, 1968. EDM—A metal removal process. Paper No. MR68-710. Dearborn, Michigan: American Society of Tool and Manufacturing Engineers.
33. American Society for Testing and Materials. Standard. methods of tension testing of metallic materials. ASTM E8. Philadephia, Pennsylvania.
34. Tentative recommended practice for conducting creep and time-for-rupture tension tests of materials. ASTM E139. Philadelphia, Pennsylvania.
35. W. K. Boyd and F. W. Fink, October 1964. The phenomenon of hot-salt stress-corrosion cracking of titanium alloys. NASA CR-117. Washington, D.C.: National Aeronautics and Space Administration.
36. American Society for Testing and Materials. Tentative method of test for plane-strain fracture toughness of metallic materials. ASTM E399. Philadephia, Pennsylvania
37. P. S. Prevey and W. P. Koster. Effect of surface integrity on fatigue of structural alloys at elevated temperatures. Cincinnati, Ohio: Metcut Research Associates Inc. Presented at the University of Connecticut, June 18-22, 1972.)
38. P.C. Paris, 1964. The fracture mechanics approach to fatigue. In *Proceedings, Tenth Sagamore Army Materials Research Conference*. Syracuse, New York: Syracuse University Press.
39. H. Johnson and P. Paris, June 1968. Subcritical flaw growth. Engineering Fracture Mechanics 1(1).
40. Edgar Berkey. Techniques for chemical analysis of engineering surfaces. (To be presented at the International Conference on Surface Technology, Pittsburgh, Pennsylvania, May 1973, sponsored by the Society of Manufacturing Engineers).
41. R. G. Goff. Ion scattering spectrometry. Journal of Vacuum Science and Technology, in press.
42. G. L. Connell and Y. P. Gupta, 1971. Auger electron spectroscopy. Materials Research and Standards 11(1): 8-13.
43. C. Nordling, March 1972. Electron spectroscopy for chemical analysis. (Paper presented at Pittsburgh Conference on Analytical Chemistry and Applied Spectroscopy.) Uppsala, Sweden: Institute of Physics.
44. C. A. Anderson and J. R. Hinthorne, February 25, 1972. Ion microprobe mass analyzer. Science 175: 853-860.